



1. Report No. FHWA/TX-92+1244-2		2. Government Accession No.		3. 7	
4. Title and Subtitle CHARACTERIZATION OF CONCRETE PROPERTIES WITH AGE				5. Report Date March 1992	
				6. Performing Organization Code	
7. Author(s) Terry Dossey and B. Frank McCullough				8. Performing Organization Report No. Research Report 1244-2	
9. Performing Organization Name and Address Center for Transportation Research The University of Texas at Austin Austin, Texas 78712-1075				10. Work Unit No. (TR AIS)	
				11. Contract or Grant No. Rsch. Study 2/3-8-90/2-1244	
12. Sponsoring Agency Name and Address Texas Department of Transportation Transportation Planning Division P. O. Box 5051 Austin, Texas 78763-5051				13. Type of Report and Period Covered Interim	
				14. Sponsoring Agency Code	
15. Supplementary Notes Study conducted in cooperation with the U. S. Department of Transportation, Federal Highway Administration. Research Study Title: "Evaluation of Performance of Texas Pavements Made with Different Coarse Aggregates"					
16. Abstract The objective of this study was to investigate the material properties of concrete made with a number of aggregates commonly used in Texas for pavement construction. This report extends the work of Project 422, which was limited to two aggregates (limestone and siliceous river gravel). Measurements taken in the laboratory were used to develop a set of equations predicting time-dependent concrete properties for the eight aggregates tested. Additional models were developed for predicting concrete behavior from the chemical composition of the aggregate, enabling a preliminary evaluation of aggregate sources to be made prior to the casting of the concrete. Inputs required for the chemical model can be obtained either from the supplier or by a quick and inexpensive laboratory test.					
17. Key Words CRCP, JRCP, elastic modulus, drying shrinkage, tensile strength, compressive strength, curing time, equivalent pavement performance, design chart			18. Distribution Statement No restrictions. This document is available to the public through the National Technical Information Service, Springfield, Virginia 22161.		
19. Security Classif. (of this report) Unclassified		20. Security Classif. (of this page) Unclassified		21. No. of Pages 50	22. Price

CHARACTERIZATION OF CONCRETE PROPERTIES WITH AGE

by

Terry Dossey
B. Frank McCullough

Research Report Number 422/1244-2

Research Project 2/3-8-90/2-1244
Evaluation of Performance of Texas Pavements Made with
Different Coarse Aggregates

conducted for the

Texas Department of Transportation

in cooperation with the

**U.S. Department of Transportation
Federal Highway Administration**

by the

CENTER FOR TRANSPORTATION RESEARCH
Bureau of Engineering Research
THE UNIVERSITY OF TEXAS AT AUSTIN

March 1992

NOT INTENDED FOR CONSTRUCTION, BIDDING, OR PERMIT PURPOSES

B. F. McCullough, P.E. (Texas No. 19914)
Research Supervisor

The contents of this report reflect the views of the authors, who are responsible for the facts and the accuracy of the data presented herein. The contents do not necessarily reflect the official views or policies of the Federal Highway Administration or the Texas Department of Transportation. This report does not constitute a standard, specification, or regulation.

PREFACE

This is the second report for Research Project 2/3-8-90/2-1244, "Evaluation of Performance of Texas Pavements Made with Different Coarse Aggregates." The research for this project was conducted at the Center for Transportation Research (CTR), The University of Texas at Austin, as part of the Cooperative Highway Research Program sponsored by the Texas Department of Transportation (TxDOT) and the Federal Highway Administration.

The purpose of this report is to summarize the findings of the Phase II testing conducted at Ferguson Laboratories under the subject project. Work was completed that compared the material properties of concrete specimens prepared with eight aggregates commonly used for pavement construction in Texas. The results of this study will be incorporated into the existing specification for steel reinforcement bars in Texas pavements.

The authors wish to express their appreciation to CTR staff and graduate students who participated in the project. Special thanks are extended to Ms. Lyn Antoniotti for preparing this manuscript, Mr. Derrick Caballero for drafting the figures, Dr. Humberto Castedo for his guidance in the preliminary stages of the analysis, and to Mr. Arthur Frakes, Ms. Kay Lee, and Ms. Jessica Salinas for their assistance in finalizing the report.

And, as always, thanks are extended to TxDOT personnel—especially Mr. James Brown—for providing guidance and cooperation.

Terry Dossey
B. Frank McCullough

LIST OF REPORTS

Report No. 422/1244-1, "Field Evaluation of Coarse Aggregate Types: Criteria for Test Sections," by Kenneth Hankins, Young-Chan Suh, and B. Frank McCullough, describes the design of the experimental test sections to be used for the verification of a design standard. The design standard is one of the first to incorporate various physical design features that account for the variety in concrete mix properties. January 1991.

Report No. 422/1244-2, "Characterization of Concrete Properties with Age," by Terry Dossey and B. Frank McCullough, presents the laboratory measurements of concrete properties for eight aggregates commonly used for pavement construction in Texas. A series of models are developed for predicting concrete property behavior, either directly from aggregate type or indirectly from the chemical composition of the aggregate. March 1992.

ABSTRACT

The objective of this study was to investigate the material properties of concrete made with a number of aggregates commonly used in Texas for pavement construction. This report extends the work of Project 422, which was limited to two aggregates (limestone and siliceous river gravel). Measurements taken in the laboratory were used to develop a set of equations predicting time-dependent concrete properties for the eight aggregates tested.

Additional models were developed for predicting concrete behavior from the chemical composition of the aggregate, enabling a preliminary evaluation of aggregate sources to be made prior to the casting of the concrete. Inputs required for the chemical model can be obtained either from the supplier or by a quick and inexpensive laboratory test.

KEYWORDS: CRCP, JRCP, elastic modulus, drying shrinkage, tensile strength, compressive strength, curing time, equivalent pavement performance, design chart.

SUMMARY

This is the fourth in a series of reports that describe studies investigating the effect of coarse aggregates on portland cement concrete (PCC) pavement performance. This report expands on the work previously reported by comparing the concrete properties of test specimens cast in the laboratory using six additional coarse aggregates commonly used in Texas (while maintaining constant curing conditions).

Subsequent analysis of the laboratory data demonstrated statistically significant differences in material properties attributed to aggregate type. Prediction models were developed that described concrete performance for each aggregate after any length of curing up to 28 days (256 days for drying shrinkage).

A second set of models was developed to predict concrete properties from the chemical composition of the aggregate, making possible a preliminary assessment of aggregate suitability prior to laboratory testing.

IMPLEMENTATION STATEMENT

Actual laboratory measurements of concrete specimens were used to develop predictive models that have been implemented in the CRCP and JRCPC computer programs. These programs can then be used to develop design charts that give equivalent pavement performance for the eight aggregates tested.

Chemical models are presented that may be used to provide a preliminary assessment of aggregate performance prior to actual laboratory testing. These models have been incorporated into a computer program for use with the IBM PC (or compatible microcomputer).

TABLE OF CONTENTS

PREFACE	iii
LIST OF REPORTS	iii
ABSTRACT	iii
SUMMARY	iv
IMPLEMENTATION STATEMENT	iv
CHAPTER 1. INTRODUCTION	
INTRODUCTION	1
BACKGROUND	1
OBJECTIVES	2
SCOPE	2
CHAPTER 2. THE DATA	
PREPARATION OF LABORATORY SPECIMENS	3
CONCRETE MATERIAL PROPERTIES	3
Compressive Strength	3
Tensile Strength	4
Modulus of Elasticity	4
Drying Shrinkage	6
CHEMICAL ANALYSIS OF THE AGGREGATES	6
Procedures	6
Results	6
CHAPTER 3. DEVELOPMENT OF DESCRIPTIVE MODELS	
INTRODUCTION	9
COMPARISON OF AGGREGATES	9
Methodology	9
Analysis of Variance	9
Multiple Comparisons (Fisher's LSD test)	9
TIME CURVES FOR TESTED AGGREGATES	11
Tensile Strength, Compressive Strength, and Elastic Modulus	11
Drying Shrinkage	11
NORMALIZED MODELS	11
Derivation	11
Results	13
Applicability	14
CHAPTER 4. CHEMICAL MODELS	
INTRODUCTION	15
METHODOLOGY	15
SELECTION OF PREDICTORS	15
REGRESSION MODELS FOR 28-DAY PROPERTIES	16
DEVELOPMENT OF TIME-DEPENDENT MODELS	18
Model 1	18
Model 2	19

DISCUSSION OF RESULTS	19
<i>Predictions for Tested Aggregates</i>	19
<i>Predictions for Untested Aggregates</i>	19
RECOMMENDATIONS	20
CHAPTER 5. USING THE MODELS	
INTRODUCTION	22
INTERPOLATION FOR TESTED AGGREGATES	22
<i>Example 1: Tensile Strength of Limestone Concrete at 21 Days</i>	22
<i>Example 2: Drying Shrinkage of Granite Aggregate at 128 Days</i>	22
USE OF NORMALIZED MODELS	22
<i>Example 3: Estimation of Curing Curve for Limestone</i>	22
<i>Example 4: Estimation of 28-Day Strength for Dolomite Aggregate</i>	23
PREDICTION FROM CHEMICAL COMPOSITION	23
<i>Example 5: Prediction of 28-Day Tensile Strength for an Unknown Aggregate</i>	23
<i>Example 6: Estimation of Curing Curve for Aggregate X</i>	23
THE CHEM PROGRAM	24
CHAPTER 6. SUMMARY AND RECOMMENDATIONS	
SUMMARY	25
RECOMMENDATIONS	25
<i>Descriptive Models</i>	25
<i>Chemical Models</i>	26
REFERENCES	27
APPENDIX A	29
APPENDIX B	37
APPENDIX C	39

CHAPTER 1. INTRODUCTION

INTRODUCTION

In the past, contractors involved in portland cement concrete (PCC) pavement construction have been allowed to choose among the different coarse aggregate types available, provided that certain gradations and other physical requirements were met (Ref 1). However, subsequent field observations have shown significant performance variance between pavements constructed with different aggregates (Ref 2).

It is now understood that aggregates indirectly affect pavement performance by directly affecting concrete material properties. Because fine and coarse aggregates account for 60 to 75 percent of the volume of cured concrete (70 to 85 percent by weight), they play a substantial role in determining the final properties of the concrete. Just as each aggregate type displays a typical compressibility, modulus of elasticity, and moisture-related shrinkage, these properties will be reflected in the strength, modulus of elasticity, and drying shrinkage of the cured concrete (Ref 3).

The environment can also affect concrete performance. For given environmental conditions, concrete volume-change stresses are affected by modulus of elasticity, thermal properties, and drying shrinkage of the concrete. These environmentally induced concrete stresses, along with wheel load stresses, depend both on the tensile strength and on the elastic modulus of the concrete, which, in turn, depend to a large extent on the type of coarse aggregate used.

BACKGROUND

Recognizing the influence of coarse aggregate type on the performance of PCC pavements, the Texas Department of Transportation (TxDOT) has sought to develop PCC pavement designs that account for such influences, as a way of ensuring the equality of pavement performance regardless of coarse aggregate selection (Ref 4). The large number of aggregate sources in the state—sand and siliceous river gravel, limestone, granite,

basalt, and sandstones can all be used for construction of concrete pavements in Texas—make these considerations important.

Most concrete pavements in Texas are constructed using either limestone or siliceous river gravel aggregate. Accordingly, Phase I of this project was restricted to lab testing and model development for limestone and siliceous river gravel aggregates (Ref 1). Although this preliminary study was limited to those two aggregate types, several combinations of temperature, humidity, and sampling times were selected to investigate the effect of curing conditions on the concrete. The design factorial for the Phase I experiment is shown in Figure 1.1.

		Moisture Conditions						
		40% Rel Humidity			100% Rel Humidity			
		Curing Temperatures						
		50°F	75°F	100°F	50°F	75°F	100°F	
Coarse Aggregate Types	Siliceous River Gravel	Curing Times	1					
		3						
		7						
		28						
		90						
	Limestone	Curing Times	1					
		3						
		7						
		28						
		90						

Figure 1.1 Factorial for Phase I laboratory testing

Using the information obtained in Phase I, the study team selected curing conditions of 75°F at 40 percent relative humidity. This decision was made to simulate curing conditions for pavements in the field, after the significance of temperature and humidity had been determined by statistical

testing. These curing conditions were then used for subsequent testing in Phase II of the project, which involved an evaluation of six additional aggregates.

OBJECTIVES

Currently, the only way to assess the effect of various aggregate materials on concrete properties is to cast concrete cylinders and physically test them in the laboratory. If the same proportion of cement, sand, water, and admixtures is used with each aggregate, and if constant environmental conditions are maintained during curing, then any resulting differences in the observed concrete properties can be attributed either to the influence of the aggregate or to normal material variability. This is the methodology of the Phase II experiment documented in this report. Using information and experience gained in Phase I, the project team tested river gravel, limestone, and six additional aggregates commonly used in Texas for pavement construction, testing their effect on concrete properties. Chapter 2 provides a description of the testing procedures, and documents the data obtained from the experiment. Descriptive models are then developed in Chapter 3 to characterize the time-dependent concrete properties for each of the tested aggregates.

However, laboratory testing of concrete is tedious and expensive. Since destructive testing is necessary, many cylinders must be cast. Moreover, as the concrete cures, the specimens must be monitored for a period ranging from 28 to 300 days; expensive environmental chambers must be used. It is therefore an additional objective of this report to present simple models for estimating

concrete properties directly from the chemical composition of the aggregate, which permits a rough comparison of aggregates prior to laboratory testing. Chapter 4 presents the results of this analysis.

Finally, through a series of examples, Chapter 5 shows how the models developed in Chapter 3 and Chapter 4 can be used to estimate time-dependent concrete properties.

SCOPE

In addition to strength and modulus of elasticity, a number of other aggregate properties affect concrete performance, including proper grading, maximum size, and surface texture (which can affect how well the cement bonds to the aggregate; see Ref 4). These considerations must remain outside the scope of this report. No deleterious aggregates were used in the study, and all aggregates tested were properly sized and graded according to TxDOT specification 360. Since an aggregate will exhibit the same chemical composition whether it is crushed or uncrushed, small or large, the chemical prediction models presented here are intended only for comparison of aggregates when all other factors are held constant.

Again, all data used to develop the models were obtained from concrete mixes made with Type I cement and cured at 75°F and 40 percent relative humidity. These curing conditions were chosen to simulate the field curing of pavements, which is the focus of this study. For that reason, the predictions may not be applicable to concrete mixtures made with other types of cement or cured under different conditions.

CHAPTER 2. THE DATA

PREPARATION OF LABORATORY SPECIMENS

All concrete data used to develop the prediction models were obtained from testing performed at the Ferguson Structural Engineering Laboratory at the Balcones Research Center, The University of Texas at Austin. Concrete specimens were prepared from each of the eight aggregates listed in Table 2.1.

To assess the effect of each aggregate on the concrete, the mix design for each cylinder, shown in Table 2.2, was held as constant as possible. All samples were cured at a constant temperature (75°F), and a constant humidity of 40 percent was chosen over moisture curing (100 percent RH) to represent more accurately the curing conditions in the field.

CONCRETE MATERIAL PROPERTIES

Testing for compressive strength, tensile strength, modulus of elasticity, and drying shrinkage was performed periodically as the concrete cured. To provide a measure of testing variability and material variance, three specimens prepared from each aggregate were tested for each curing time period.

Compressive Strength (f_c)

Compressive strength was determined after 1, 3, 7, and 28 days of curing, according to the procedure documented in ASTM C-39 (Ref 7), which consists of the application of a continuous compressive axial load to the molded concrete

Table 2.1 Coarse aggregates used in Project 422 (Ref 6)

<u>Aggregate</u>	<u>Source</u>	<u>TxDOT District</u>	<u>County</u>
SRG	Fordyce Gravel Chipley Pit	13	Victoria
LS	Texas Crushed Stone/Feld Pit	14	Williamson
VG	Vega Sand and Gravel/Tom Green Pit	4	Oldham
WT	Western Sand and Gravel/Tascosa Pit	4	Oldham
FR	Texas Industries/Ferris Plant	2	Parker
DL	El Paso Sand Products/McKelligon Canyon	24	El Paso
GR	TXTX Aggregates/Scotland		
BTT	50/50 blend of:		
	Texas Industries/Bridgeport	2	Wise
	Texas Industries/Tin Top Plant #539	2	Parker

Table 2.2 Mix design of the concrete specimens (weights in lb/yard³) (Ref 5)

<u>Item</u>	<u>SRG^a</u>	<u>LS^a</u>	<u>GR^a</u>	<u>DL^a</u>	<u>FR^a</u>	<u>VG^a</u>	<u>WT^a</u>	<u>BTT^a</u>
Cement	492	492	492	492	492	492	492	492
Sand	1,023	1,279	1,228	1,228	1,228	1,228	1,228	1,228
Aggregate ^b	2,148	1,838	1,966	2,967	1,970	1,955	1,970	1,997
Water	226	222	224	224	224	224	224	224
Air entr (oz)	3.4	2.5	2.7	2.7	2.7	2.7	2.7	2.7
Air (%)	4.8	4.8	4.5	5	4	4.75	4.5	4.5
Slump (in.)	1.5	1.5	1.75	1.75	2.75	1	1.5	2

^aSee Table 2.1 for aggregate source.

^bAggregate weights vary because of different specific gravities. Mix was by volume.

Table 2.3 Compressive strength (psi)

Aggregate Type ^a	Sample	1 Day	3 Days	7 Days	28 Days
SRG	1	1,510	2,822	4,128	4,779
	2	1,270	2,902	4,298	4,937
	3	1,374	2,750	4,015	4,896
LS	1	1,277	2,729	3,951	4,922
	2	1,176	2,706	3,695	4,817
	3	1,193	2,830	3,917	5,259
GR	1	1,506	2,792	4,040	4,996
	2	1,474	2,801	3,796	5,077
	3	1,291	2,809	3,549	4,828
DL	1	1,343	2,678	3,356	4,408
	2	1,837	3,507	4,626	3,942
	3	1,167	2,535	4,028	5,045
FR	1	1,592	2,676	3,475	4,010
	2	1,405	2,642	3,630	4,012
	3	1,487	2,805	3,532	3,945
VG	1	915	2,822	4,008	4,674
	2	1,077	2,875	2,622	3,343
	3	953	2,941	4,239	-
WT	1	1,396	2,949	3,869	4,222
	2	1,344	2,609	3,534	3,950
	3	1,304	2,848	3,461	4,246
BTT	1	1,163	2,877	3,260	4,104
	2	1,123	2,493	3,285	3,796
	3	1,255	3,074	3,993	4,380

^aSee Table 2.1 for aggregate source.
 - Test not performed.

cylinders at a prescribed rate until failure. Table 2.3 summarizes the results.

Tensile Strength (*f_t*)

Tensile strength was also measured at 1, 3, 7, and 28 days using a split cylinder test specified in ASTM C-496 (Ref 7). Simply put, this test involves applying a load over the entire length of the specimen and then recording the maximum load indicated at failure. The tensile strength is calculated by the formula

$$f_t = \frac{2P}{\pi ld}$$

where:

- f_t* = splitting tensile strength (psi),
- P = maximum applied load (lb),
- l = length (in.), and
- d = diameter (in.).

Data for each replicate are given in Table 2.4.

Modulus of Elasticity (*E*)

Concrete modulus of elasticity was tested after the same curing period used by the compressive and tensile strength tests. Following a procedure reported in ASTM C-469 (Ref 6), elastic moduli were calculated from longitudinal deformations under continuous compressive loading using the following equation:

$$E = \frac{(S_2 - S_1)}{(e_2 - 0.00005)}$$

where:

- E = chord modulus of elasticity (psi),
- S₂ = 40 percent ultimate stress value,
- S₁ = stress corresponding to strain of 50 millionths (psi), and
- e₂ = longitudinal strain produced by stress S₂.

Results appear in Table 2.5.

Table 2.4 Splitting tensile strength (psi)

Aggregate Type^a	Sample	1 Day	3 Days	7 Days	28 Days
SRG	1	208	286	431	463
	2	156	232	465	445
	3	175	258	435	458
LS	1	183	268	431	389
	2	195	269	367	398
	3	183	283	376	510
GR	1	–	336	398	486
	2	221	319	482	551
	3	199	402	437	551
DL	1	197	317	470	533
	2	238	363	444	506
	3	227	436	448	442
FR	1	259	394	313	466
	2	258	322	383	501
	3	238	361	402	460
VG	1	107	334	464	442
	2	79	255	349	463
	3	93	310	405	419
WT	1	225	301	378	458
	2	245	313	361	388
	3	241	345	375	450
BTT	1	190	352	365	462
	2	176	306	461	452
	3	177	332	454	408

^aSee Table 2.1 for aggregate source.

– Test not performed.

Table 2.5 Elastic modulus (psi, millions)

Aggregate Type^a	Sample	1 Day	3 Days	7 Days	28 Days
SRG	1	3.395	4.206	4.716	4.397
	2	3.858	4.323	4.556	4.172
	3	3.858	3.939	4.301	4.119
LS	1	2.498	2.829	3.537	3.691
	2	2.832	3.115	3.493	3.731
	3	2.927	3.265	3.389	3.691
GR	1	2.572	3.203	3.409	3.537
	2	2.738	3.203	3.075	3.420
	3	2.497	3.144	3.215	3.458
DL	1	2.978	4.577	4.390	4.491
	2	2.695	3.612	3.979	4.964
	3	3.773	4.446	4.391	5.144
FR	1	3.075	3.537	3.837	4.135
	2	2.978	3.537	3.903	4.073
	3	3.368	3.612	3.836	4.135
VG	1	1.121	2.497	2.663	4.042
	2	2.497	3.753	3.426	3.858
	3	2.234	3.395	3.593	3.745
WT	1	2.460	2.874	3.482	3.628
	2	2.695	3.203	3.430	3.840
	3	2.358	2.966	3.482	3.409
BTT	1	2.695	3.858	3.773	3.773
	2	2.460	3.691	3.903	4.287
	3	2.978	3.691	3.836	4.223

^aSee Table 2.1 for aggregate source.

Drying Shrinkage (Z)

The final property considered for modeling was drying shrinkage. Since considerable shrinkage continued beyond the 28-day limit used for the other tests, and since testing for shrinkage is non-destructive, measurements were continued for 256 days or more. The drying shrinkage was then determined using a modification of the ASTM C-157 test method (Ref 7), in which three sets of demec points were epoxied onto each cylinder, each set being aligned with the longitudinal axis of the cylinder and each placed 120° apart along the circumference of the cylinder. Two companion cylinders were stored, yielding six sets of demec points from which shrinkage readings were taken. A 200-mm demec gauge having an accuracy of ± 8.1 microstrains was used to take the shrinkage readings. Table 2.6 reports the shrinkage for each sample (Ref 8).

CHEMICAL ANALYSIS OF THE AGGREGATES

Procedures

Samples of the eight aggregates used in the concrete specimens, along with an additional eleven untested aggregates (Table 2.7, bottom), were sent for chemical assay to the Bureau of Economic Geology's Mineral Study Laboratory (MSL) at The University of Texas at Austin. Prior to analysis, each sample was pulverized to a powder using a riffle sample splitter followed by a tungsten carbide shatterbox. Oven drying at

105°C was used to eliminate residual moisture. Three tests were then performed on each aggregate: (1) a mineral composition test (determined by x-ray diffraction); (2) an oxides test (measured by a fusion process, MSL procedure SWI 1.5); and (3) a coulometric test for mineral carbon (SWI 1.7).

Results

Results of the mineralogical testing and chemical analysis were in agreement, and yielded the findings presented in Table 2.7 and the chemical compositions in Table 2.8. As expected, the samples displayed a wide range of chemical composition. The river gravels used in the study exhibited a high silicate content (ranging from 67 to 94 percent) and a low carbonate content (less than 10 percent). Conversely, the limestones and dolomites were low in silicates and high in carbonates.

Prior to modeling, two additional samples of aggregate, including their chemical analysis, were received (Ref 10). These samples, provided by Boorhem-Fields, Inc., consisted of sandstone from a pit near Apple, Oklahoma. Because this aggregate is chemically very different from the others in the study, and since it had been used in the recent construction of IH-30 in Sulphur Springs, Texas, it is included in Table 2.8.

Table 2.9 shows the percentage range of chemical components determined in the analysis for the eight tested aggregates. These ranges will limit the inference space of the chemical prediction models presented in Chapter 3.

Table 2.6 *Drying shrinkage (Z) 10⁻⁶ inch/inch (average for two specimens)*

Gravel (SRG)		Limestone (LS)		Granite (GR)		Dolomite (DL)		Ferris (FR)		Vega (VG)		W. Tascosa (WT)		Brg/TTop (BTT)	
Day	Z	Day	Z	Day	Z	Day	Z	Day	Z	Day	Z	Day	Z	Day	Z
0	0	0	0	1	0	1	0	1	0	1	0	1	0	1	0
1	30	1	24	3	69	2	47	2	41	3	32	3	45	2	29
4	48	3	21	6	132	3	56	3	90	7	66	8	64	4	48
6	71	6	57	7	150	6	63	7	115	12	110	10	115	6	73
12	117	13	123	11	193	7	79	10	163	14	133	15	120	11	117
20	160	20	166	14	235	10	87	15	225	19	192	18	164	18	140
26	182	34	217	17	260	15	111	18	261	26	217	24	207	20	170
39	214	57	268	25	280	17	126	21	277	28	227	28	216	25	190
62	246	84	334	30	311	22	158	29	309	68	359	52	294	28	220
89	270	126	375	55	328	29	183	56	338	92	398	91	355	62	319
131	296	256	424	91	353	60	240	90	354	121	410	162	404	101	356
256	352 ^a			136	364	95	282	141	373	180	435	244	414	172	376
262	355			207	382	125	307	213	399	252	456	256	417 ^a	244	398
				247	395	183	319	253	417	256	457 ^a	274	421	256	400 ^a
				256	396 ^a	255	333	256	418 ^a	292	464	339	435	349	419
				312	404	256	333 ^a	318	431	357	478				
						295	345								

^aBy linear interpolation.

Table 2.7 *Mineralogical results (x-ray diffraction)*

Source	Aggregate Type	Minerals Found		
		Most Abundant	Second	Third
McKelligon Canyon #1	DL	Dolomite	Calcite	Quartz
Western-Tascosa	WT	Quartz	Calcite	
Tin-Top #1	BTT	Calcite	Quartz	
Bridgeport	BTT	Calcite	Dolomite	Quartz
Feld (TCS)	LS	Calcite	Dolomite	Quartz
Fordyce	SRG	Quartz	Calcite	
Vega	VG	Quartz	Calcite	
Ferris #1	FR	Calcite	Quartz	
Scotland Granite	GR	Quartz	Albite	
TXI-Boonesville	BO	Calcite	Quartz	
McKelligon Canyon #2	DL2	Dolomite	Calcite	Quartz
Ferris #2	FR2	Calcite	Quartz	
TCP-Cleburne #51	CL	Calcite	Quartz	
Ingram Whitehead	IW	Calcite	Quartz	
TXI-Tin Top #2	TT2	Calcite	Quartz	
Pioneer-Landess Pit	PI	Calcite	Quartz	
Jobe-Hueco	JH	Calcite	Quartz	
Rainbour-Baker Pit	RB	Calcite	Quartz	
A-Rock Brazos River Pit	BR	Calcite	Quartz	
Vulcan-Mexico	VM	Calcite	Quartz	

Table 2.8 Coarse aggregate chemical analysis data—Research Study 422 (Ref 9)

Source	Aggregate Type	SiO ₂	CaO	MgO	CO ₂	MnO	Fe ₂ O ₃	Al ₂ O ₃	Na ₂ O	K ₂ O	TiO ₂	Other
McKelligon	Dolomite (DL)	6.53	34.9	13.0	42.9	.02	0.21	0.38	0.09	0.26	0.02	1.69
Western-T	S/L (WT)	68.5	11.4	0.35	8.98	.05	2.64	3.97	0.85	1.1	0.17	1.99
Bridpt+Tin Top	L+S/L (BTT*)	17.53	42.55	0.71	35.65	0.04	0.57	0.56	0.15	0.30	0.04	1.91
Feld (TCS)	Limestone (LS)	2.56	45.7	5.97	43.3	.01	0.06	0.21	0.14	0.21	0.02	1.82
Fordyce	SRG (SRG)	93.8	2.23	0.11	1.77	.01	0.76	0.63	0.18	0.32	0.1	0.09
Vega	SRG (VG)	66.9	11.6	0.39	9.07	.07	2.33	4.22	0.95	1.16	0.19	3.12
Ferris	L/S (FR)	14.2	42.1	0.43	34.4	.10	3.70	0.87	0.17	0.26	0.06	3.71
Scotland	Granite (GR)	71.3	1.5	0.63	0.59	.03	1.52	14.3	4.4	3.83	0.29	1.61
TXI-Boonesville	(BO)	5.26	49.8	0.34	40.0	0.03	0.40	0.41	0.06	0.14	0.02	3.54
McKelligon Canyon #2	(DL2)	7.31	35.2	12.4	42.8	0.02	0.21	0.42	0.11	0.29	0.03	1.21
Ferris #2	(FR2)	12.5	42.8	0.44	35.4	0.10	3.56	0.76	0.17	0.28	0.06	3.93
TCP-Cleburne #51	(CL)	18.8	41.3	0.49	34.7	0.05	0.72	0.62	0.19	0.31	0.04	2.78
Ingram Whitehead	(IW)	23.9	38.7	0.44	31.2	0.05	0.77	0.69	0.21	0.32	0.05	3.67
TXI-Tin Top #2	(TT2)	33.6	34.1	0.35	27.9	0.06	0.91	0.74	0.16	0.32	0.05	1.81
Pioneer-Landess Pit	(PI)	14.7	42.8	0.42	34.7	0.09	3.31	0.65	0.15	0.25	0.05	2.88
Jobe-Hueco	(JH)	17.5	41.7	1.62	35.1	0.02	0.45	1.01	0.16	0.35	0.06	2.03
Rainbow-Baker Pit	(RB)	32.8	34.6	0.41	27.9	0.06	0.98	0.69	0.21	0.36	0.05	1.94
A-Rock Brazos River Pit	(BR)	55.6	20.2	0.43	16.4	0.03	0.89	2.31	0.64	0.93	0.11	2.46
Vulcan-Mexico	(VM)	0.27	53.1	0.55	43.8	0.01	0.03	0.23	0.18	0.28	0.04	1.51
Sandstone - Sample 1	(SA1)	97.5	0.07	0.02	•	•	1.03	0.55	0.12	0.05	0.02	0.66
Sandstone - Sample 2	(SA2)	96.0	0.10	0.04	•	•	2.01	0.55	0.12	0.10	0.02	1.10

*These aggregates combined in a 50/50 blend when tested in the laboratory for concrete properties.

•Sample was not tested for these compounds.

Table 2.9 Percentage of chemical components

Compound	Range	
	High	Low
SiO ₂	93.8	2.56
CaO	45.7	1.50
MgO	13.0	0.11
CO ₂	42.9	0.59
MnO	0.1	0.01
Fe ₂ O ₃	3.7	0.06
Al ₂ O ₃	14.3	0.21
Ma ₂ O	4.4	0.09
K ₂ O	3.8	0.21
TiO ₂	0.29	0.02
Other	3.71	0.09

CHAPTER 3. DEVELOPMENT OF DESCRIPTIVE MODELS

INTRODUCTION

The tables presented in Chapter 2 clearly show differences in observed performance among the concrete specimens cast from the eight tested aggregates. The tables also show a considerable variance between cylinders cast from the same aggregate and tested at the same age: a result of (1) the normal variability of materials found even in cement and aggregate from the same batch, and (2) the difficulty in precisely repeating laboratory procedures. Using statistical analysis, it is possible to separate random variance from experimental factors to determine which aggregates are significantly different in terms of concrete performance. The first part of this chapter provides a statistical comparison of aggregates.

Once a significant difference among aggregates has been established, simple descriptive models can be calculated to provide curing curves for the concrete properties of each aggregate observed in the laboratory. These curves can then be used to estimate concrete properties at any curing time t within the time period covered by the experiment. The second part of this chapter presents these time-dependent models.

COMPARISON OF AGGREGATES

Methodology

The standard statistical technique for determining the significance of differences between groups is hypothesis testing (Ref 11). In this instance, it was necessary to determine whether the observed differences in the material properties of concrete specimens made with different aggregates are greater than would be expected to occur by chance. This is expressed by the following two hypotheses:

$$H_0: \bar{x}_1 = \bar{x}_2 = \bar{x}_3 = \dots \bar{x}_8$$

and

H_a : at least two means are different

where H_0 is the null hypothesis that suggests that the population mean for a given concrete property is the same for all aggregates; H_a is the alternate hypothesis that not all of the means are the same; and $\bar{x}_1 - \bar{x}_8$ are the population means for f_t , f_c , E , and Z for each of the eight aggregates.

Analysis of Variance

The standard statistical procedure for hypothesis testing is analysis of variance (ANOVA). Performing an ANOVA for each of the four material tests yielded the results shown in Table 3.1.

A common reference probability frequently seen in the literature is $p = 0.05$, which corresponds to 95 percent confidence. Using this standard, it can be said with 95 percent confidence that, whenever the p value in Table 3.1 is less than 0.05, the null hypothesis can be rejected, which indicates a significant difference between levels of the test variable. Applying this method to Table 3.1, it is apparent that curing time is a significant factor in all four tests, that the aggregate type is significant for all tests, and that the interaction between curing time and aggregate is significant only for tensile strength and drying shrinkage.

Multiple Comparisons (Fisher's LSD Test)

Now that it has been shown that significant differences exist among the tested aggregates, we must next investigate which aggregates are significantly different by using a multiple comparison procedure. Two types of parametric tests are available for such an investigation; results from one commonly used test—Fisher's Least Significant Difference test (LSD)—are presented here. The LSD test can be used to perform multiple t -tests, controlling the comparison-wise error rate (CER), while other techniques control the experiment-wise error rate (MEER) (Ref 11). From a practical standpoint, controlling the CER means that each decision of significance between pairs of

aggregates is made with 95 percent confidence, but the probability that at least one incorrect decision between pairs will be made is greater than 5 percent.

Table 3.1 ANOVA results for tested aggregates

Property	Predictor	F-Value	P > F
f_c ($r^2 = 0.96$ $n = 95$)	Time	451.49	0.0001
	Aggregate	3.80	0.0017
	Time * Agg	1.61	0.0745
f_t ($r^2 = 0.94$ $n = 95$)	Time	283.82	0.0001
	Aggregate	7.74	0.0001
	Time * Agg	3.01	0.0004
E ($r^2 = 0.86$ $n = 96$)	Time	63.38	0.0001
	Aggregate	26.08	0.0001
	Time * Agg	1.67	0.0612
Z ($r^2 = 0.99$ $n = 64$)	Time	682.74	0.001
	Aggregate	30.43	0.0001
	Time * Agg	8.36	0.0001

f_c = compressive strength E = modulus of elasticity
 f_t = tensile strength Z = drying shrinkage

Table 3.2 shows the results of the LSD test for 28-day compressive strength (f_c). Aggregates grouped with the same letter cannot be said to be significantly different at the 95 percent confidence level. Thus, in terms of compressive strength, the aggregates divided into two fairly distinct groups, with limestone (LS), granite (GR), and river gravel (SRG) each yielding a significantly higher f_c than Western-Tascosa (WT), Bridgeport-Tin Top (BTT), Vega (VG), and Ferris (FR). Placement of dolomite (DL) aggregate could not be determined at the $\alpha = 0.05$ level.

Table 3.2 Comparison of means for 28-day compressive strength

Grouping*	Mean (psi)	N	Aggregate
A	4,999.3	3	LS
A	4,967.0	3	GR
A	4,870.7	3	SRG
B A	4,465.0	3	DL
B	4,139.3	3	WT
B	4,093.3	3	BTT
B	4,008.5	2	VG
B	3,989.0	3	FR

*Means with the same letter are not significantly different. Least significant difference = 634.98 for $\alpha = 0.05$.

Table 3.3 gives the results for 28-day tensile strength (f_t). GR aggregate exhibited the greatest strength after 28 days' curing, showing a mean f_t of 529 psi versus 494 psi for the next strongest aggregate, DL. However, since the least significant difference was 66 psi, GR was not shown to be significantly different from DL and FR.

Table-3.3 Comparison of means for 28-day tensile strength

Grouping*	Mean (psi)	N	Aggregate
A	529.33	3	GR
B A	493.67	3	DL
B A	475.67	3	FR
B	441.33	3	SRG
B	455.33	3	VG
B	440.67	3	BTT
B	432.33	3	LS
B	432.00	3	WT

*Means with the same letter are not significantly different. Least significant difference = 65.6 for $\alpha = 0.05$.

Table 3.4 shows comparisons among 28-day elastic moduli (E) for the eight aggregates. Dolomite has the highest 28-day modulus (4.87)—significantly higher (at the 95 percent confidence level) than all of the other aggregates tested. The rest of the table requires a more complex interpretation. For instance, while SRG was found to have a significantly higher modulus than WT, GR, or LS, it did not prove significantly different from FR, BTT, or VG aggregates.

Table 3.4 Comparison of means for 28-day elastic modulus

Grouping*	Mean (psi)	N	Aggregate
A	4.8663	3	DL
B	4.2293	3	SRG
B	4.1143	3	FR
C B	4.0943	3	BTT
C B D	3.8817	3	VG
C E D	3.6257	3	WT
E D	3.4717	3	GR
E	3.3710	3	LS

*Means with the same letter are not significantly different. Least significant difference = 0.488 for $\alpha = 0.05$.

The final comparison table (Table 3.5) shows that GR and FR aggregates exhibit significantly higher 28-day drying shrinkage (Z) than the other six aggregates, possibly a result of lower water

absorption. The lowest 28-day drying shrinkage was developed by DL, giving a Z value of 157 microstrains versus 330 for GR. The least significant difference determined by Fisher's LSD for Z was 43 microstrains, which corresponds to a 95 percent confidence level.

Table 3.5 Comparison of means for 28-day drying shrinkage

Grouping*	Mean (in./in. 10 ⁻³)	N	Aggregate
A	329.50	2	GR
A	316.50	2	FR
B	227.00	2	VG
B	216.50	2	WT
C B	205.50	2	LS
C B D	186.50	2	SRG
C D	170.00	2	BTT
D	156.50	2	DL

*Means with the same letter are not significantly different. Least significant difference = 43.0 for $\alpha = 0.05$.

TIME CURVES FOR TESTED AGGREGATES

Now that a difference in aggregate performance has been demonstrated, individual curves can be fitted to the laboratory points in order to model f_t , f_c , E, and Z as a function of curing time for each aggregate. After examining the literature and testing several possible models, we selected the following form (Ref 15):

$$F(t) = A(2 - e^{-Bt} - e^{-Ct}) \quad (3.1)$$

where:

t = the time of curing (days),

F(t) = the concrete property (f_t , f_c , E, or Z) at time t, and

A, B, and C = coefficients of curvature specific to a given aggregate, given in Table 3.6.

Tensile Strength, Compressive Strength, and Elastic Modulus

Using the above equation and the replicate data points obtained from laboratory testing, values for A, B, and C were estimated by nonlinear least squares regression; these are given for each aggregate in Table 3.6. The use of three regression parameters (A, B, and C) resulted in an excellent fit, in which R^2 values were no lower than 0.96 for any of the material properties across all aggregates. Because Equation 3.1 was developed simply

to describe the laboratory results within the limited inference space of eight aggregates and a 28-day curing period, overfitting of the data was not a concern.

Using the coefficients given in these tables, the tensile strength and modulus of elasticity can be reliably estimated for any of the eight tested aggregates at any time t up to 28 days. Figures 3.1 to 3.3 compare the calculated f_c , f_t , and E values for the eight tested aggregates, while more detailed plots showing the fit of Equation 3.1 to the laboratory data for each aggregate can be found in Appendix A.

Drying Shrinkage

Using Equation 3.1, a model was also calculated for drying shrinkage (Z) curves (Ref 15)—in this case developed from 256 days of data rather than 28 days, in order to better model long-term shrinkage. As for the f_c , f_t , and E models, R^2 values were very high, ranging from 0.95 to 1.0 across the aggregates.

Coefficients for calculating drying shrinkage using Equation 3.1 are given in Table 3.6. Figure 3.4 contrasts the calculated drying shrinkage curves for the aggregates, while graphs for each aggregate, showing the fit to the laboratory points, are given in Appendix A.

NORMALIZED MODELS

Derivation

As shown above, Equation 3.1 can be used to determine absolute values for tensile strength, compressive strength, modulus of elasticity, and drying shrinkage for each of the eight tested aggregates. However, in order to estimate the strength, modulus, or shrinkage of PC concrete at a curing time t relative to a chosen "final" curing time t_f , a normalized model is required. Using a t_f of 28 days for tensile strength, compressive strength, and elastic modulus, and a t_f of 256 for drying shrinkage, normalized models were developed from Equation 3.1 by dividing the A coefficient given in Table 3.6 by the value of the respective material property at curing time t_f , resulting in the following equations:

$$F_N(t) = N_{28}(2 - e^{-Bt} - e^{-Ct}) \quad (3.2)$$

$$Z_N(t) = N_{256}(2 - e^{-Bt} - e^{-Ct}) \quad (3.3)$$

where:

t = the time of curing (days),

Table 3.6 Coefficients for Equations 3.1, 3.2, and 3.3 (Ref 15)

		GR	DL	VG	BTT	WT	FR	LS	SRG
Compressive strength (f_c)	A	2,570.8	2,236.7	1,995.3	2,038.2	2,068.5	2,000.1	2,550.57	2,445.25
	B	0.096	0.231	0.367	0.582	0.214	0.206	0.115	0.182
	C	0.623	0.562	0.367	0.220	0.647	0.801	0.490	0.473
	N ₂₈	0.5176	0.5009	0.4978	0.4980	0.4998	0.5014	0.5102	0.5020
Tensile strength (f_t)	A	266.46	247.06	221.08	221.85	216.01	241.94	217.83	231.07
	B	0.15	0.261	0.302	0.332	0.198	0.137	0.177	0.267
	C	1.05	1.094	0.3014	0.723	2.505	2.479	1.068	0.468
	N ₂₈	0.504	0.500	0.500	0.500	0.501	0.505	0.502	0.500
Elastic modulus (E)	A	1.678	2.324	1.882	1.992	1.803	1.979	1.802	2.282
	B	0.78	0.485	0.301	0.688	0.405	0.738	0.535	0.574
	C	1.65 x 10 ¹⁴	3.537	1.574	2.00	97.056	2.668 x 10 ¹²	110.46	61,755.1
	N ₂₈	0.500	0.500	0.500	0.500	0.500	0.500	0.500	0.500
Drying shrinkage (Z)	A	321.23	252.06	235.19	343.62	358.456	327.23	229.1	198.39
	B	0.0851	0.04062	0.3948	0.0328	0.3109	0.0745	0.0398	0.0619
	C	0.001	0.00155	0.01255	0.00069	0.000715	0.00119	0.00754	0.005
	N ₂₈	0.8112	0.7569	0.5146	0.8582	0.8600	0.7828	0.5403	0.5636

$F_N(t)$ = the normalized concrete property (f_t , f_c , or E) at time t ,

$Z_N(t)$ = the normalized drying shrinkage at time t , and

N_{28} , N_{256} , B , and C = coefficients of curvature specific to each aggregate, given in Table 3.6.

Equation 3.2, which ranges from 0 at $t = 0$ to 1 at $t = 28$, should be used to calculate normalized tensile strength, compressive strength, and modulus of elasticity. Equation 3.3, normalized at 256 days, is used only for drying shrinkage.

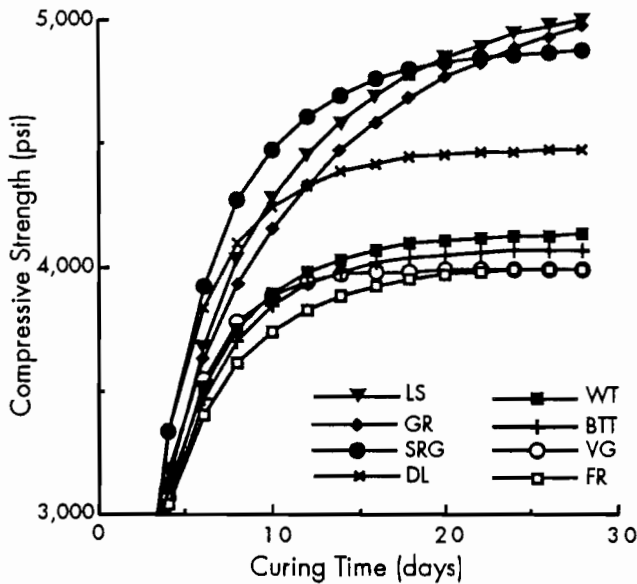


Figure 3.1 Curing curves for compressive strength (from Eq 3.1)

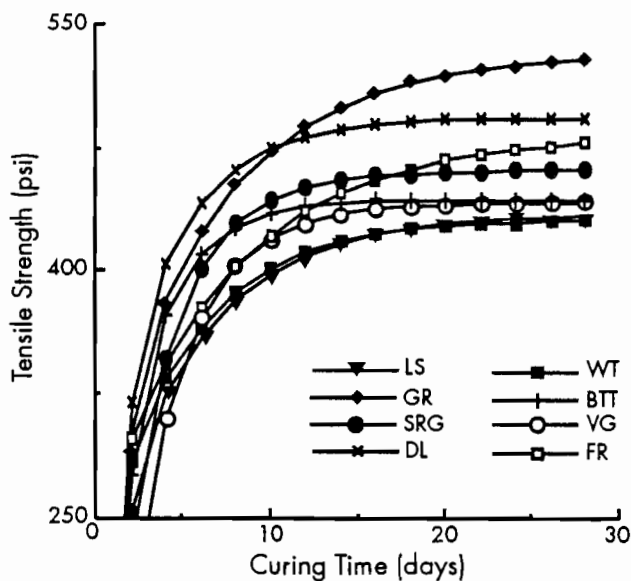


Figure 3.2 Curing curves for tensile strength (from Eq 3.1)

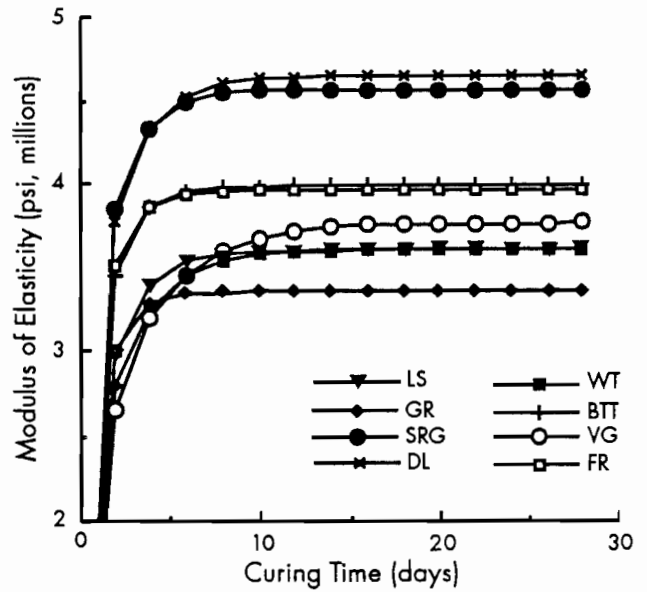


Figure 3.3 Curing curves for elastic modulus (from Eq 3.1)

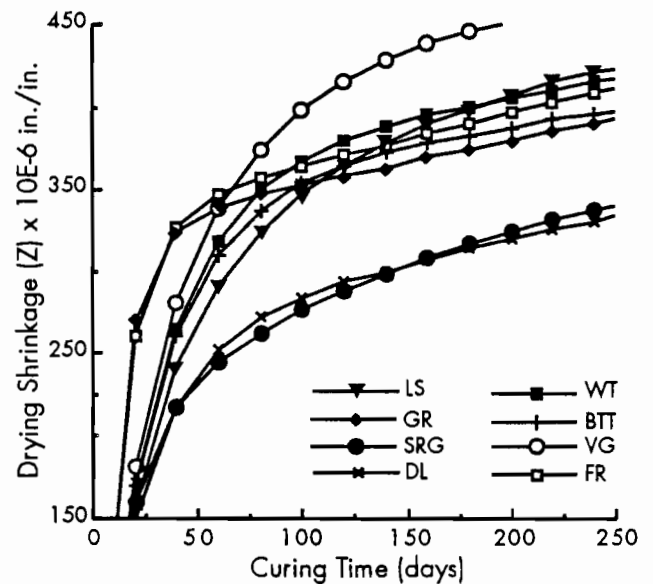


Figure 3.4 Curing curves for drying shrinkage (from Eq 3.1)

Results

Figure 3.5 shows the relative rates at which a concrete specimen prepared from limestone aggregate attains its 28-day compressive strength, tensile strength, and modulus of elasticity. As shown by the figure, the elastic modulus reaches its final value more rapidly than tensile strength or compressive strength.

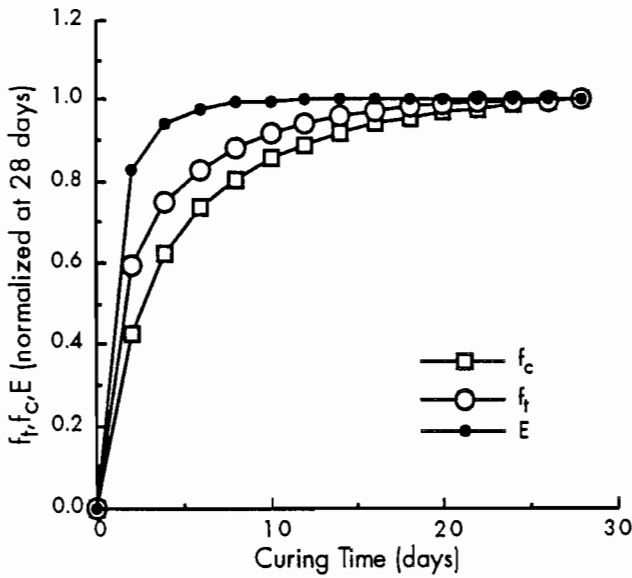


Figure 3.5 Normalized material properties for limestone aggregate (from Eq 3.2)

Figure 3.6 compares the drying shrinkage rate of limestone concrete with concrete made with granite (GR) aggregate. Since the limestone is porous, it holds moisture longer and retards the rate at which the shrinkage develops. By contrast, granite is not very absorptive, causing a rapid rate of shrinkage.

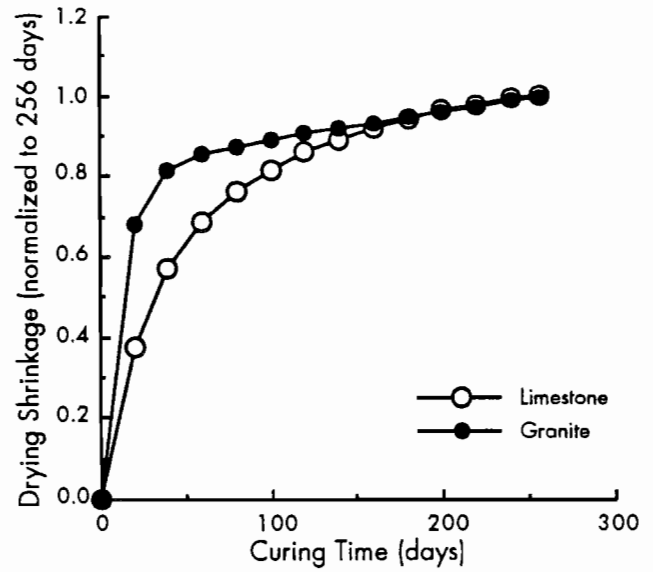


Figure 3.6 Normalized shrinkage rates for limestone and granite aggregates (from Eq 3.3)

Applicability

These normalized models are applicable only for predicting properties of pavement concrete made with the aggregates listed in Table 2.1, cured at 40 percent relative humidity at 75°F. The reliability of the models is directly related to the degree of precision and repeatability of the various laboratory test procedures used to determine the concrete properties being studied. A description of the laboratory test procedures is given in Chapter 2.

CHAPTER 4. CHEMICAL MODELS

INTRODUCTION

As explained in Chapter 3, the models presented thus far are descriptive in nature; that is, they describe mathematically the relationships between concrete properties and curing time for eight aggregates that have undergone material testing in the laboratory. However, they cannot predict properties for concrete made from aggregates that have not yet been tested.

Since concrete testing is expensive and tedious, requiring as it does many specimens cast and cured over an extended period of time, a simple and inexpensive test that predicts the performance of an aggregate based on its chemical composition would be very useful for the preliminary evaluation of aggregates. Such a model is presented here.

METHODOLOGY

It is generally accepted that the curing rate of concrete is primarily dependent on the type of cement used and on the temperature and humidity conditions experienced during curing (Ref 4); the use of different types of coarse aggregate will therefore have a greater effect on the final strength of the concrete. Since all the concrete specimens cast in Phase II of the study were mixed and cured under identical conditions, curing rates should be similar for all specimens; any differences in the final properties (excluding normal material variances and laboratory test repeatability) can be attributed to aggregate influence. For this reason, only Phase II data will be used in the analysis.

The first phase of the analysis predicts 28-day material properties from chemical composition. Because drying shrinkage develops more slowly, and because long-term shrinkage data are available from the Phase II study, 256-day shrinkage was used instead of the 28-day values. Chemical

composition data from the laboratory analysis (given in Table 2.8) can be used to predict 28-day (or 256-day) material properties using multiple regression techniques.

SELECTION OF PREDICTORS

Since concrete properties were tested for only the first eight aggregates, there are insufficient degrees of freedom to use all ten chemical components, much less their interactions, in a standard analysis of variance (ANOVA). Instead, as a preliminary step, a correlation analysis was undertaken to determine which chemicals are interdependent. Even though concrete specimens were prepared for only the first 8 aggregates in Table 2.8, all 21 aggregates under study have been assayed and were used to investigate chemical associations. Correlation was determined using the Pearson product-moment correlation (Ref 11), in which the correlation r_{xy} between x and y is given by

$$r_{xy} = \frac{\sum(x - \bar{x})(y - \bar{y})}{\sqrt{(\sum(x - \bar{x})^2 \sum(y - \bar{y})^2)}}$$

where \bar{x} and \bar{y} are the sample means.

The results of this analysis are given in Table 4.1 (Ref 12). Strong positive correlations are rendered in boldface, indicating that the chemicals belong to the following groups, probably as they exist as ores in nature:

Group 1	Group 2	Group 3	Group 4	Group 5
SiO ₂	CaO	MgO	Fe ₂ O ₃	Al ₂ O ₃
	CO ₂		MnO	TiO ₂
				Na ₂ O
				K ₂ O

Table 4.1 Correlations among chemical components

Compound	SiO ₂	TiO ₂	Al ₂ O ₃	Fe ₂ O ₃	MnO	MgO	CaO	Na ₂ O	K ₂ O	CO ₂
SiO ₂	1.00	0.45	0.37	0.19	-0.05	-0.39	-0.97	0.33	0.32	-0.98
TiO ₂	0.45	1.00	0.91	0.30	0.05	-0.26	-0.54	0.87	0.92	-0.87
Al ₂ O ₃	0.37	0.91	1.00	0.18	-0.03	-0.15	-0.49	0.99	0.99	-0.67
Fe ₂ O ₃	0.19	0.30	0.18	1.00	0.88	-0.39	-0.17	0.12	0.13	-0.27
MnO	-0.05	0.05	-0.03	0.88	1.00	-0.40	0.11	-0.08	-0.08	-0.02
MgO	-0.39	-0.26	-0.15	-0.39	-0.40	1.00	0.20	-0.13	-0.12	0.44
CaO	-0.97	-0.54	-0.49	-0.17	0.11	0.19	1.00	-0.45	-0.45	0.95
Na ₂ O	0.33	0.87	0.99	0.12	-0.08	-0.13	-0.45	1.00	0.99	-0.63
K ₂ O	0.32	0.92	0.99	0.13	-0.08	-0.12	-0.45	0.99	1.00	-0.67
CO ₂	-0.98	-0.87	-0.67	-0.27	-0.02	0.44	0.95	-0.63	-0.67	1.00

Further examination of Table 4.1 reveals a strong *negative* correlation between groups 1 and 2, indicating that, whenever SiO₂ is present in high concentration, CaO and CO₂ are not. This correlation was expected, since siliceous aggregates generally have low carbonate content. For statistical purposes, this result means that it would be unnecessary to include both groups in the analysis.

Based on the above observations, regressors from groups 2 through 5 were selected, using the compound present in highest concentration to represent each group. Thus, CaO, MgO, Fe₂O₃, and Al₂O₃ were selected as primary regressors. CaO was chosen over CO₂ because a significant portion of the CO₂ was released during the high temperature analysis from the CaMg(CO₃)₂ (dolomite) present in some aggregates. This effect is confirmed by the partial positive correlation (r = .44) between CO₂ and MgO shown in Table 4.1.

REGRESSION MODELS FOR 28-DAY PROPERTIES

Considering the four primary regressors selected above and their two-way interactions, the RSQUARE procedure of the SAS statistics package (Ref 13) was used to determine the five best one-, two-, and three-variable models for 28-day tensile strength (f_t), compressive strength (f_c), modulus of elasticity (E), and 256-day drying shrinkage (Z). The RSQUARE procedure is similar to a stepwise regression but calculates the quality of fit for every possible combination of predictors. Although time-consuming, this method is superior to stepwise regression because RSQUARE always finds the best possible models (based on high R value) regardless of the order in which the variables are entered.

Drying shrinkage was predicted at 256 days because laboratory measurements were available for all eight tested aggregates at that time. Models were restricted to three or fewer predictors to

avoid the overfitting (and consequent low predictive ability) associated with models having few remaining degrees of freedom. Table 4.2 shows an excerpt from Ref 12 of the best one-, two-, and three-variable models found, while Table B.1 (Appendix B) shows the SAS program used to perform this analysis.

Selecting a model from Table 4.2 for each of the concrete properties and then calculating regression coefficients results in the following models:

$$f_t(28) = -59.238 \cdot \ln(\text{CaO}) + 46.884 \cdot \ln(\text{MgO}) + 1.7159 \frac{\text{CaO}}{\text{MgO}} + 572.2 \quad (4.1)$$

$$f_c(28) = -403.2 \cdot \ln(\text{CaO}) + 6.806 \frac{\text{CaO}}{\text{Al}_2\text{O}_3} + 5120.5 \quad (4.2)$$

$$E(28) = -0.4135 \cdot \ln(\text{Al}_2\text{O}_3) + 0.264 \cdot \ln(\text{MgO}) - 0.00948 \frac{\text{CaO}}{\text{Al}_2\text{O}_3} + 4.664 \quad (4.3)$$

$$Z(256) = 1.8723(\text{CaO} \cdot \text{Al}_2\text{O}_3) + 0.1223 \frac{\text{CaO}}{\text{Fe}_2\text{O}_3} - 0.1383(\text{CaO} \cdot \text{MgO}) + 350.6 \quad (4.4)$$

For compressive strength, the two-variable model was chosen for simplicity over the three-variable model because the additional predictor would have added only an insignificant amount to the goodness of fit (see Table 4.2). Scattergrams plotting the predicted 28-day (or 256-day) properties versus the mean laboratory findings are given as Figures 4.1 through 4.4. All fits were excellent, with R² values ranging from a low of 0.95 (for shrinkage) to a high of 0.98 (for compressive strength). (Complete details of the analysis of variance and regression modeling can be found in Ref 11.)

Table 4.2 Best models found for 28-day properties

Property	Best 1 Variable Model		Best 2 Variable Model		Best 3 Variable Model	
	Predictors	R ²	Predictors	R ²	Predictors	R ²
f _t	MgO • Al ₂ O ₃	0.717	MgO • Al ₂ O ₃ CaO • Fe ₂ O ₃	0.834	CaO MgO CaO/MgO	0.970
f _c	CaO • Al ₂ O ₃	0.627	CaO CaO/Al ₂ O ₃	0.961	CaO • Al ₂ O ₃ CaO CaO/Al ₂ O ₃	0.983
E	Al ₂ O ₃ • Fe ₂ O ₃	0.445	Al ₂ O ₃ • Fe ₂ O ₃ MgO • Fe ₂ O ₃	0.789	Al ₂ O ₃ MgO CaO/Al ₂ O ₃	0.969
Z	CaO • Al ₂ O ₃	0.522	CaO • Al ₂ O ₃ MgO • Fe ₂ O ₃	0.739	CaO • Al ₂ O ₃ CaO/Fe ₂ O ₃ CaO • MgO	0.948

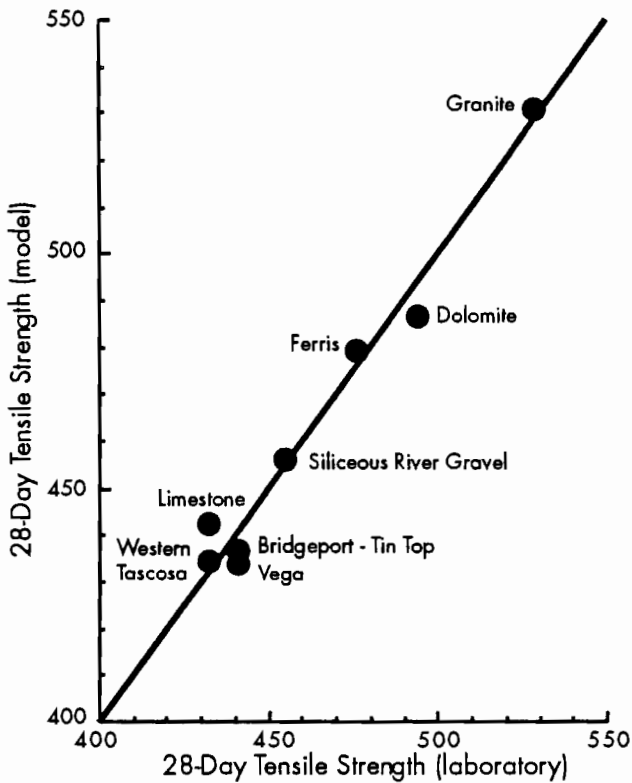


Figure 4.1 Predicted versus observed tensile strength

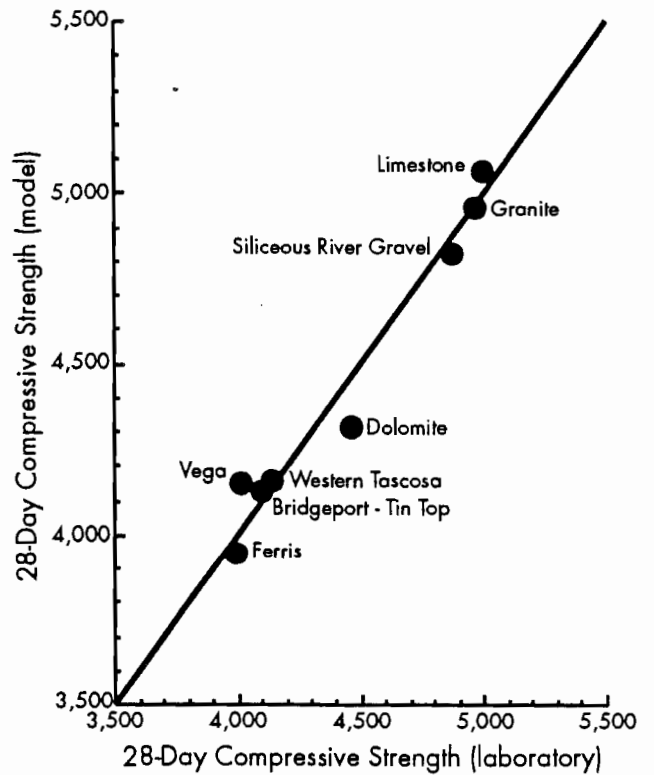


Figure 4.2 Predicted versus observed compressive strength

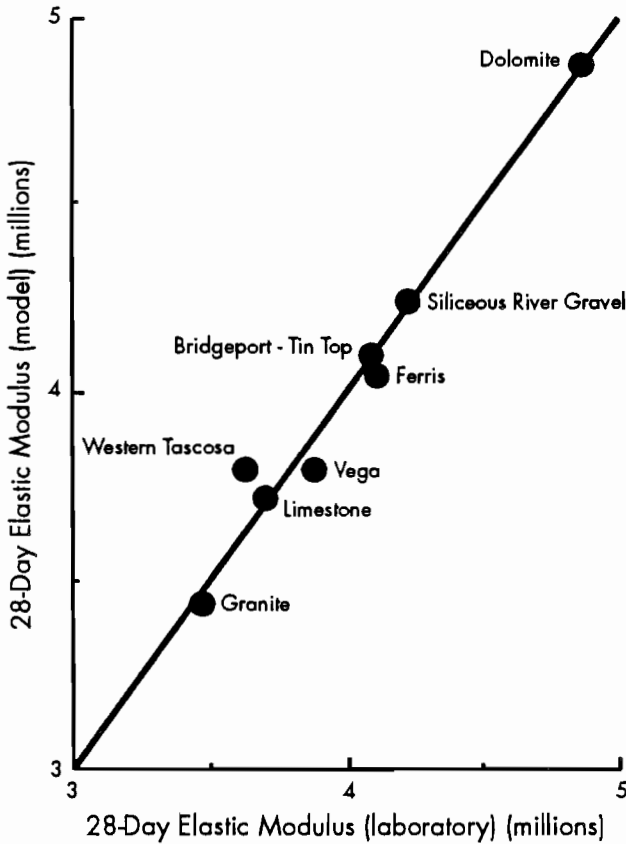


Figure 4.3 Predicted versus observed elastic modulus

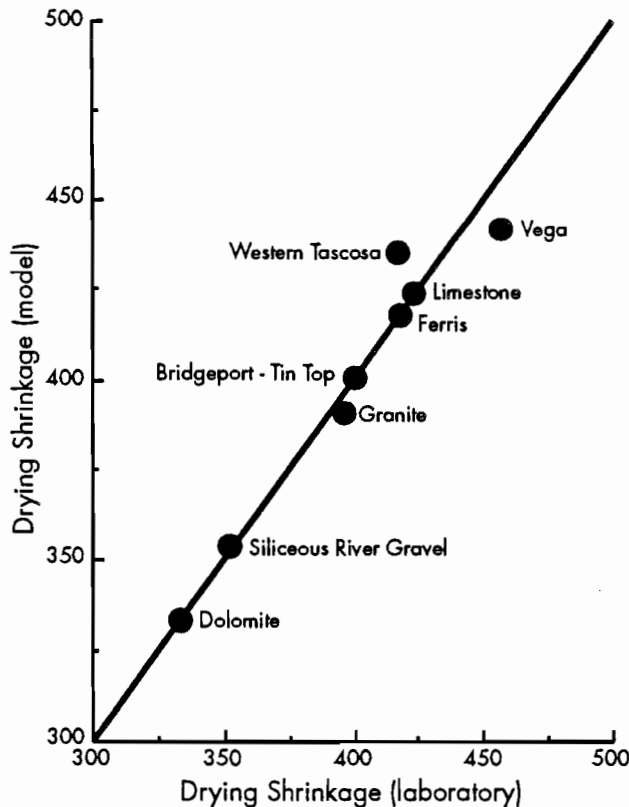


Figure 4.4 Predicted versus actual drying shrinkage

DEVELOPMENT OF TIME-DEPENDENT MODELS

In addition to the development of 28-day models, a method is needed for estimating any of the material properties after a given curing time t . If concrete curing time is assumed to be independent of coarse aggregate type, all that remains is to calculate a normalized curing curve for each of the material properties and then adjust it for each aggregate using the 28-day (256-day for Z) values predicted by the equations above. Four curing models were tried, and the best two are presented below.

Model 1

Won (Ref 4) developed the following model, which relates compressive strength at time t as a percentage of the 28-day compressive strength for Type I cement moisture-cured at 70°F:

$$f_c(t) = f_c(28) \frac{t}{(4 + .85t)} \quad (4.5)$$

Because the specimens used in this study were cured at a lower relative humidity (40 percent), it is necessary to adjust the slope of Equation 4.5. In the general form, this equation becomes

$$F(t) = F(28) \frac{t}{(A + Bt)} \quad (4.6)$$

where F is the concrete property function (f_c , f_t , E , or Z) at time t , and A and B are coefficients of curvature, which can be determined by multiple regression techniques. Coefficients for Equation 4.6 can also be determined for tensile strength, elastic modulus, and drying shrinkage. Using the multivariate secant method of nonlinear least squares regression (Ref 12), the following curing curves were obtained, averaged for all aggregates:

$$f_c(t) = f_c(28) \frac{t}{(2.1743 + 0.90597t)} \quad (4.7)$$

$$f_t(t) = f_t(28) \frac{t}{(1.43139 + 0.94156t)} \quad (4.8)$$

$$E(t) = E(28) \frac{t}{(0.43056 + 0.99451t)} \quad (4.9)$$

$$Z(t) = Z(256) \frac{t}{(23.851 + 0.91056t)} \quad (4.10)$$

The SAS program for this procedure is given in Table C.2.

Model 2

The second most successful form, adapted from another one of the models tried in the study (Ref 13), is:

$$F(t) = F(28)(A)(2 - e^{-Bt} - e^{-Ct})$$

Again, combining data from all aggregates, and finding a least squares fit for A, B, and C, yields the following property curves:

$$f_c(t) = f_c(28)(0.50136)(2 - e^{-.57677t} - e^{-.17658t}) \quad (4.11)$$

$$f_t(t) = f_t(28)(0.50189)(2 - e^{-.19901t} - e^{-1.0597t}) \quad (4.12)$$

$$E(t) = E(28)(0.89032)(2 - e^{-.004799t} - e^{-1.5282t}) \quad (4.13)$$

$$Z(t) = Z(256)(0.52452)(2 - e^{-.067464t} - e^{-.00984t}) \quad (4.14)$$

DISCUSSION OF RESULTS

Predictions for Tested Aggregates

For the eight aggregates tested for concrete properties, direct comparisons can be made between prediction models and observed data. Figure 4.5 compares the predictions from all the models presented herein for tensile strength of limestone concrete. It can be seen from the figure that all three models fit well within the experimental scatter of the data. In general, there is little observed difference between the two chemical models, Model 1 and Model 2.

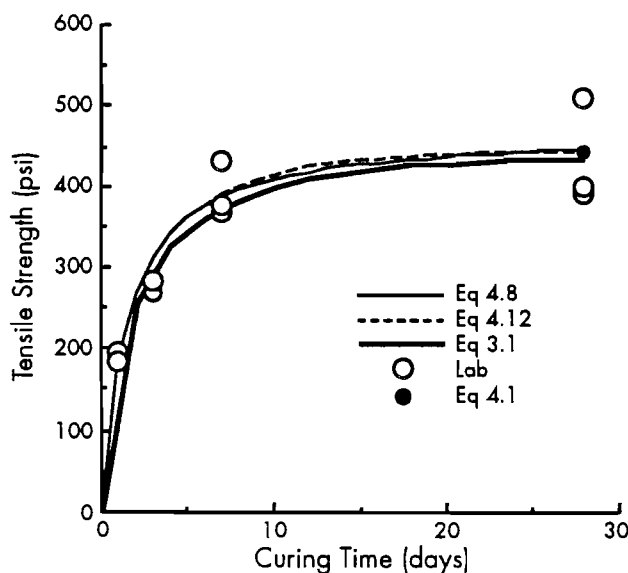


Figure 4.5 Tensile strength of limestone

Figure 4.6, a graph of elastic modulus for concrete made with SRG aggregate, demonstrates a basic difference between the chemical and descriptive models. The descriptive model presented in Chapter 3 minimizes the mean square error over all observed points, predicting a 28-day modulus that is higher than observed. By contrast, the chemical models implicitly place a heavy weight on the final values, predicting the 28-day modulus perfectly but providing a poorer fit for earlier curing times. This anomaly is a function of the variability of the laboratory testing and is present in only a small portion of the data. Comparison figures for all aggregates and concrete properties are included in Appendix A.

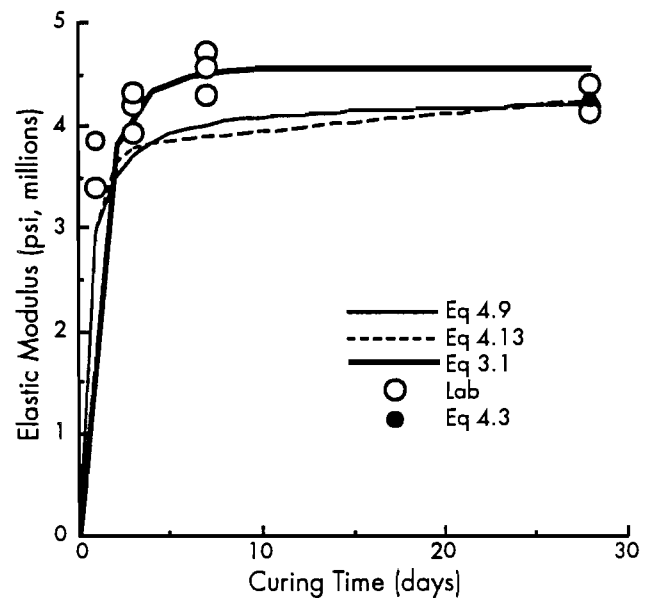


Figure 4.6 Elastic modulus of siliceous river gravel

Predictions for Untested Aggregates

Unlike the descriptive models presented in Chapter 3, the chemical models may be used to predict concrete properties for untested aggregates, provided chemical composition data are available. In many cases, this information may be obtained directly from the aggregate supplier; failing that, an inexpensive series of chemical tests may be performed (as described in Ref 9).

Figures 4.7 through 4.10 show the concrete properties predicted by Model 1 for the 11 untested aggregates. Using only the chemical composition data from Table 2.8 resulted for the most part in very reasonable predictions. It must be stressed, however, that several of these aggregates had chemical compositions at or outside the limits of the inference space used in model development (Table 2.9). The aggregate obtained from

Vulcan Materials (VM), markedly different from the other aggregates used in calibrating the model, has been omitted from some of the figures. Predictions for aggregates such as these are more likely to be inaccurate.

RECOMMENDATIONS

When carefully applied within the inference space of the models (Table 2.9), either Model 1 or Model 2 can be used to provide a fast and inexpensive preliminary assessment of aggregate performance. Of course, it is recommended that standard concrete testing procedures be followed before any final decision is made regarding aggregate suitability.

Since laboratory testing has been conducted on only eight aggregates to date, testing of additional aggregates is needed to improve the fit and expand the inference space of the model. At the time of this writing, chemical and material testing is being undertaken, and improved chemical models are expected to be developed from the supplemental data.

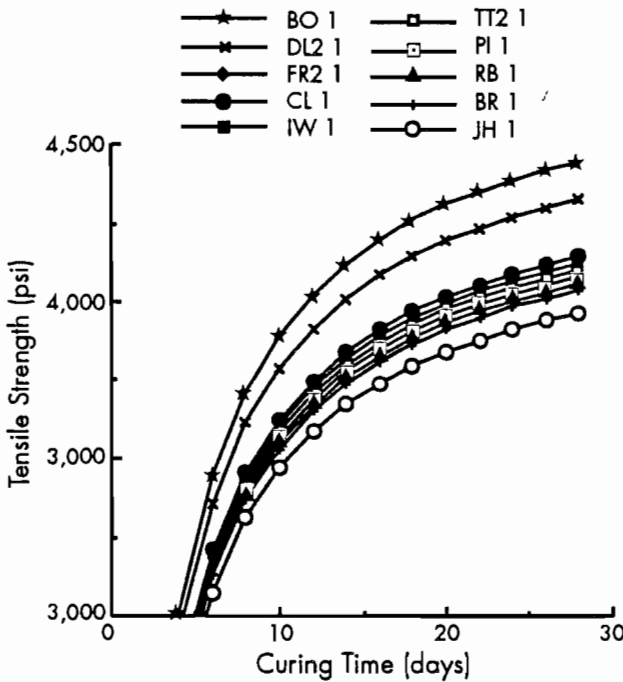


Figure 4.7 Predicted compressive strength for untested aggregates (Model 1)

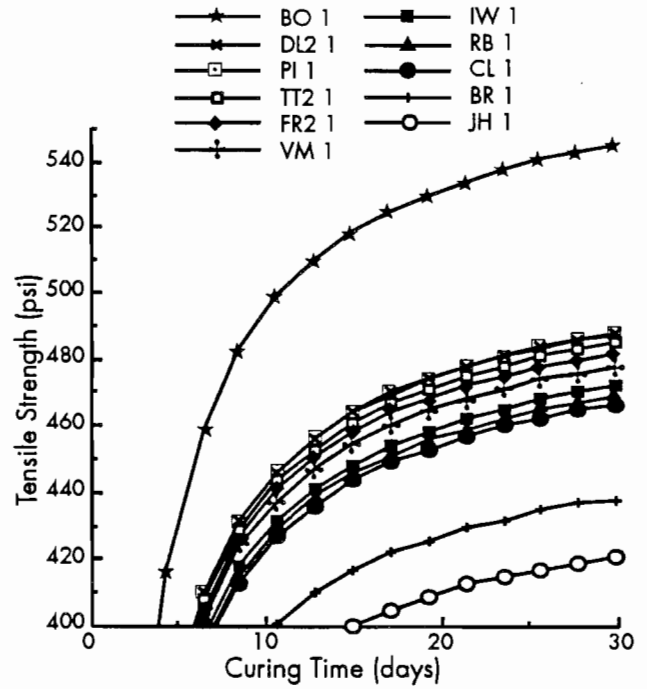


Figure 4.8 Predicted tensile strength for untested aggregates (Model 1)

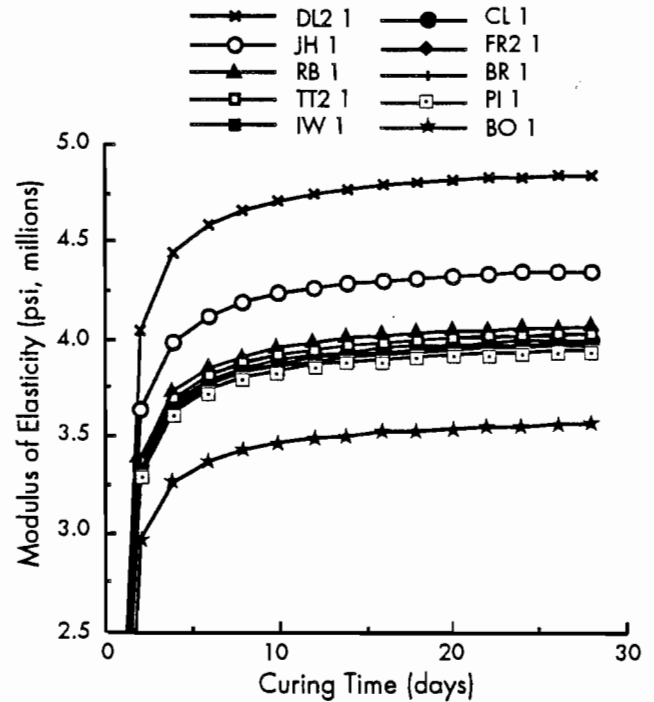


Figure 4.9 Predicted elastic modulus for untested aggregates (Model 1)

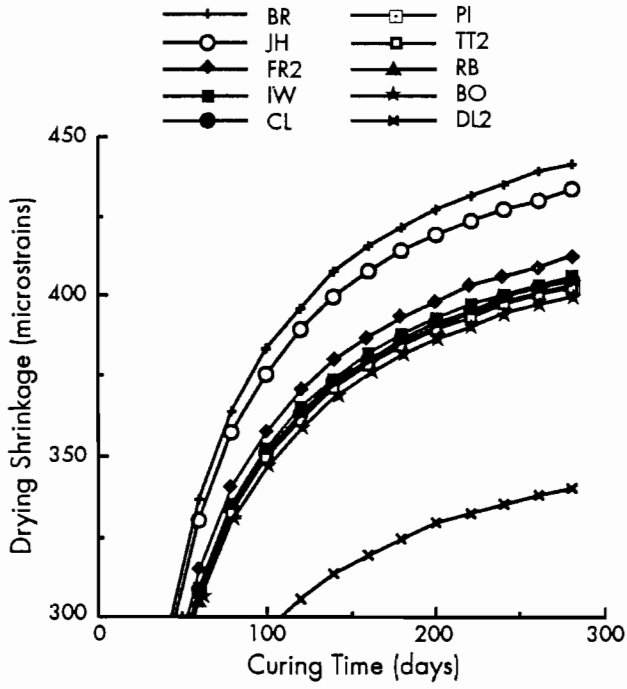


Figure 4.10 Predicted drying shrinkage for untested aggregates (Model 1)

CHAPTER 5. USING THE MODELS

INTRODUCTION

In Chapters 3 and 4, a total of 15 models were presented for predicting concrete material properties. Each model has its own specific uses and limitations. While the models presented in Chapter 3 are very accurate, they can predict concrete properties only for the eight aggregates that were tested in the study. The chemical models presented in Chapter 4 can be used to predict concrete properties for untested aggregates, but they must be carefully applied within the chemical inference space of the models. In this chapter, examples are given for some typical prediction model applications.

INTERPOLATION FOR TESTED AGGREGATES

If an estimate of compressive strength, tensile strength, elastic modulus, or drying shrinkage for any of the eight aggregates in Table 2.1 is desired, Equation 3.1 may be used. Any curing time t between 0 and 28 days (256 days for drying shrinkage) may be selected. (It should be remembered that all the models assume curing at 75°F and a 40 percent relative humidity.)

Example 1: Tensile Strength of Limestone Concrete at 21 Days

Equation 3.1 gives the equation for any concrete property at $t = 21$ days as

$$f_t(21) = A (2 - e^{-B(21)} - e^{-C(21)})$$

Table 3.6 gives the coefficients for tensile strength of limestone as $A = 217.8$, $B = 0.177$, and $C = 1.068$. Therefore, f_t at 21 days is

$$\begin{aligned} f_t(21) &= 217.8 (2 - e^{-0.177(21)} - e^{-1.068(21)}) \\ &= 217.8 (2 - 0.0243 - 0.000) \\ &= 217.8 (1.976) \\ &= 430 \text{ psi} \end{aligned}$$

This is confirmed by Figure A.14.

Example 2: Drying Shrinkage of Granite Aggregate at 128 Days

In the drying shrinkage section, Table 3.6 gives $A = 321.2$, $B = 0.085$, and $C = 0.001$ for granite. Following the same procedure as in Example 1, the 128-day shrinkage is estimated to be

$$\begin{aligned} Z(128) &= 321.2 (2 - e^{-0.085(128)} - e^{-0.001(128)}) \\ &= 321.2 (2 - 0.00 - 0.88) \\ &= 360 \text{ microstrains} \end{aligned}$$

This result is confirmed by Figure A.32.

USE OF NORMALIZED MODELS

If an aggregate is similar to one of the eight aggregates listed in Table 2.1, and if the 28-day strength or modulus is known (or 256-day shrinkage), either Equation 3.2 or 3.3 can be used to estimate the curing curve back to the time of placement. Chapter 3 explains how these models were derived.

Example 3: Estimation of Curing Curve for Limestone

A PCC concrete using limestone aggregate has a 28-day compressive strength of 5,000 psi; a curing curve is needed to estimate strength at earlier ages. Table 2.1 shows that the most comparable aggregate tested in the study was a limestone supplied by Texas Crushed Stone in Williamson County, Texas. Table 3.6 gives the coefficients for the limestone-normalized compressive strength model as $N_{28} = 0.510$, $B = 0.115$, and $C = 0.49$. Plugging A , B , and C into Equation 3.2 and multiplying by the 28-day strength gives

$$f_c(t) = 0.51(5000) (2 - e^{-0.115t} - e^{-0.49t}) \quad (5.1)$$

Thus, the above equation estimates f_c at any time t up to 28 days. Figure 5.1 shows a plot of the results.

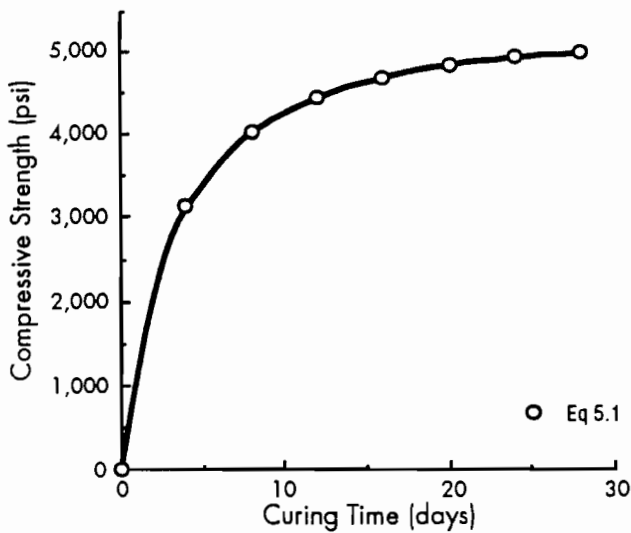


Figure 5.1 Results from Example 3

Example 4: Estimation of 28-day Strength for Dolomite Aggregate

A dolomite aggregate used to cast a concrete specimen cured at 75°F and 40 percent relative humidity displays an elastic modulus of 4.2 million psi after 7 days. To estimate what the modulus will be at 28 days, Equation 3.2 can be used to calculate the ratio of the 7-day modulus to the 28-day modulus, that is,

$$\begin{aligned} \frac{E_7}{E_{28}} &= N_{28}(2 - e^{-Bt} - e^{-Ct}) \\ &= 0.5(2 - e^{-0.485(7)} - e^{-3.537(7)}) \\ &= 0.5(2 - 0.0335 - 0.00) \\ &= 0.98 \end{aligned}$$

and, since the concrete has attained 98 percent of its 28-day modulus at 7 days, the estimated modulus at 28 days would be

$$\begin{aligned} E_{28} &= \frac{4.2 \times 10^6 \text{ psi}}{0.98} \\ &= 4.3 \times 10^6 \text{ psi} \end{aligned}$$

PREDICTION FROM CHEMICAL COMPOSITION

Chapter 4 presented prediction models for estimation of concrete properties from the chemical composition of the aggregate. These models

are not intended as a substitute for concrete testing but may be used as a tool for preliminary evaluation of a proposed aggregate prior to lab testing.

Example 5: Prediction of 28-day Tensile Strength for an Unknown Aggregate

Chemical analysis of a proposed aggregate yields the following chemical composition (percent by weight):

Aggregate X:	41.7 percent CaO
	2.76 percent MgO
	1.01 percent Al ₂ O ₃
	0.10 percent Fe ₂ O ₃
	54.4 percent other

From the high CaO content, the sample would appear to be a limestone (since MgO content is low, it cannot be a dolomite). Crystallography shows the most common mineral to be calcite, which confirms that the sample is limestone. Equation 4.1 estimates the 28-day tensile strength f_{t28} :

$$\begin{aligned} f_{t28} &= -59.2 \ln(\text{CaO}) + 46.9 \ln(\text{MgO}) + 1.72 \frac{\text{CaO}}{\text{MgO}} + 572 \\ &= -221 + 23 + 26 + 572 \\ &= 400 \text{ psi} \end{aligned}$$

Example 6: Estimation of Curing Curve for Aggregate X

Using the 28-day tensile strength (f_{t28}) predicted in Example 5, a curing curve can be drawn showing the development of tensile strength with age. Two methods are available, the first of which uses Equation 4.8:

$$f_t(t) = f_{t28} \frac{t}{1.43 + 0.942t} \quad (5.2)$$

which, as explained in Chapter 4, is the generalized curing curve for tensile strength derived from Phase II testing. Since the aggregate is known to be a limestone, an alternative approach could use Equation 3.2 with the coefficients for limestone from Table 3.6:

$$\begin{aligned} f_t(t) &= (f_{t28})(N_{28})(2 - e^{-Bt} - e^{-Ct}) \\ &= (400 \text{ psi})(0.502)(2 - e^{-0.177t} - e^{-1.068t}) \\ &= (201 \text{ psi})(2 - e^{-0.177t} - e^{-1.068t}) \quad (5.3) \end{aligned}$$

Figure 5.2 compares the curing curves obtained for Example 6 by the two methods.

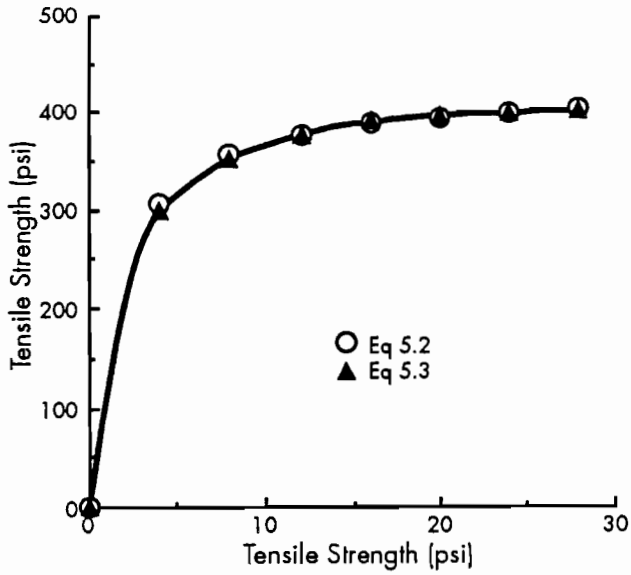


Figure 5.2 Results from Example 6

THE CHEM PROGRAM

For convenience in applying the chemical prediction models presented in Chapter 4, a user-friendly computer program, CHEM, has been developed for the IBM personal computer (and its compatibles). CHEM is written in BASIC and may be compatible with or adaptable to other computers as well. The program requests percentage by weight of four key chemical components and then draws predicted curing curves for tensile strength, compressive strength, elastic modulus, and drying shrinkage according to Model 1 presented in Chapter 4. CHEM, included as Appendix C, may be obtained on diskette from the authors.

CHAPTER 6. SUMMARY AND RECOMMENDATIONS

SUMMARY

This report documents the Phase II findings of Project 422/1244. Previously, the subject study had been confined to examining the properties of concrete mixtures prepared using limestone and siliceous river gravel aggregates. Phase II expands the study to include six additional aggregates commonly used for PCC pavement construction in Texas. As a result of findings from the Phase I study, the range of concrete curing conditions employed in Phase II was narrowed to a single environment of 75°F at 40 percent relative humidity; this decision was based on tests of statistical significance, as well as on a desire to simulate conditions found in the field.

Chapter 2 documents the Phase II data collected from concrete testing and chemical analysis, including the testing procedures utilized. Differences in aggregate performance were apparent in the data, as was the considerable experimental variability.

Chapter 3 describes the statistical techniques employed to determine whether differences between aggregates in terms of tensile strength, compressive strength, modulus of elasticity, and drying shrinkage were greater than could be expected to occur by chance, and concludes that aggregate choice was found to influence significantly all of the above material properties at the 95 percent confidence level. Rate of curing was found to be independent of aggregate selection to a greater extent than either drying shrinkage or tensile strength.

Next, a multiple comparison procedure was employed to determine which aggregates were significantly different from the average for each material property tested. Although the results require complex interpretation (given in Chapter 3), a few basic conclusions can be drawn:

- (1) Limestone, granite, and siliceous river gravel specimens exhibited significantly higher 28-day compressive strength than the other aggregates tested.
- (2) Granite, dolomite, and Ferris specimens displayed the highest 28-day tensile strengths. The tensile strength of granite was significantly higher than all the other aggregates, except dolomite and Ferris.
- (3) A single aggregate, dolomite, was found to have a 28-day modulus of elasticity that was significantly higher than that of all the other aggregates tested.
- (4) For drying shrinkage, granite and Ferris aggregates exhibited the highest shrinkage at 28 days: a result that was significantly higher than that of all the other aggregates.

After differences in aggregate performance were demonstrated, regression models were developed to describe the time-dependent characteristics of each aggregate. Following a literature review, new forms for the models were adapted, which resulted in fits better than those associated with the models used in the previous Phase I study. Normalized models were also developed to aid in adaptation to concrete cured under different conditions.

Chapter 4 investigates the prediction of concrete material properties from aggregate chemical composition. Input to the model consists of chemical percentages (by weight) that can usually be obtained from the aggregate supplier, or, alternately, from a simple and inexpensive lab test. Presence of oxides of calcium (CaO), magnesium (MgO), iron (Fe₂O₃), and aluminum (Al₂O₃) were found to be correlated to concrete material properties.

Chapter 5 contains sample applications of the 15 models presented in the previous chapters. A computer program, CHEM, has been developed to apply the chemical prediction models developed in Chapter 4. This program, which works on IBM PCs and compatibles, has been included as Appendix C. (It is also available on diskette.)

RECOMMENDATIONS

Descriptive Models

The descriptive models presented in Chapter 3 are immediately useful for describing the

time-dependent concrete properties of the eight aggregates studied. In particular, the CRCP and JRC computer programs currently used for determining steel requirements in CRC and JRC pavements can be improved by inclusion of these new models. Work is presently underway to incorporate these new models; documentation of the revisions and their results will be included in a later report.

Chemical Models

The prediction of concrete properties from the chemical composition of the aggregate is a new and promising area of study. Preliminary results

indicate that such predictions are feasible, but it must be remembered that the models presented in Chapter 4 are based solely on the eight aggregates for which complete concrete testing was performed. Consequently, the model's inference space is strictly limited by the range of chemical components in the tested aggregates. For instance, although many limestones are purer (have higher calcium oxide content) than the limestone in the study (45.7 percent CaO), the model cannot reliably predict for them. It is expected that additional aggregates currently being tested will provide data that can be used to expand the inference space and improve the predictive ability of the models.

REFERENCES

1. Aslam, M., C. L. Saraf, R. Carrasquillo, and B. F. McCullough, "Design Recommendations for Steel Reinforcement of CRCP," Research Report 422-2, Center for Transportation Research, The University of Texas at Austin, November 1987.
2. Gutierrez de Velasco, M., and B. F. McCullough, "Summary Report for 1978 CRCP Condition Survey in Texas," Research Report 177-20, Center for Transportation Research, The University of Texas at Austin, January 1981.
3. Kosmatka, S. H., and W. C. Panarese, "Design and Control of Concrete Mixtures," Portland Cement Association, Thirteenth Edition, 1988, pp 30-40.
4. Won, M., "Mechanistic Analysis of Continuously Reinforced Concrete Pavements Considering Materials Characteristics, Variability, and Fatigue," Ph.D. diss., Department of Civil Engineering, The University of Texas at Austin, May 1989.
5. MacGregor, J. G., *Reinforced Concrete, Mechanics and Design*, Prentice Hall, 1988.
6. Castedo, H., "Summary of Laboratory Test Results, Phases I and II - Project 422," Center for Transportation Research Tech Memo 422-47, The University of Texas at Austin, January 1989.
7. 1985 Annual Book of ASTM Standards, Section 4, Construction, Vol 04.02, Concrete and Mineral Aggregates.
8. Castedo, H., and T. Dossey, "Proposed Drying Shrinkage (Z) Prediction Models for Pavement Concrete Made with Various Coarse Aggregate," Center for Transportation Research Tech Memo 422-50, The University of Texas at Austin, February 1989.
9. Tweedy, S. W., "Analysis Report R-121-87," Mineral Studies Laboratory, Bureau of Economic Geology, The University of Texas at Austin, 1987.
10. Hankins, K., "Location of a CRCP Project with Sandstone CA in the Concrete Paving," Center for Transportation Research Tech Memo 422-53, The University of Texas at Austin, October 1988.
11. Snedecor, G. W., and W. C. Cochran, *Statistical Methods*, 6th ed., Iowa State University Press, 1967.
12. Dossey, T., "Prediction of Concrete Properties from Aggregate Chemical Assay," Center for Transportation Research Tech Memo 422-58, The University of Texas at Austin, May 1989.
13. SAS Institute Inc., *SAS User's Guide: Statistics, Version 5 Edition*, Cary NC: SAS Institute, Inc., 1985.
14. Lu, J., H. Castedo, and B. F. McCullough, "Normalization of Models 1 and 2 for Tensile Strength, Modulus of Elasticity, and Drying Shrinkage Made with Texas Coarse Aggregates," Center for Transportation Research Tech Memo 422-38, The University of Texas at Austin, February 1989.
15. Lu, J., "Summary of Tech Memos 422-35(a) and 422-35(b) and Recommendations of Model Based on Various Criteria," Center for Transportation Research, The University of Texas at Austin, September 1988.

APPENDIX A. PREDICTION OF CONCRETE PROPERTIES FOR TESTED AGGREGATES

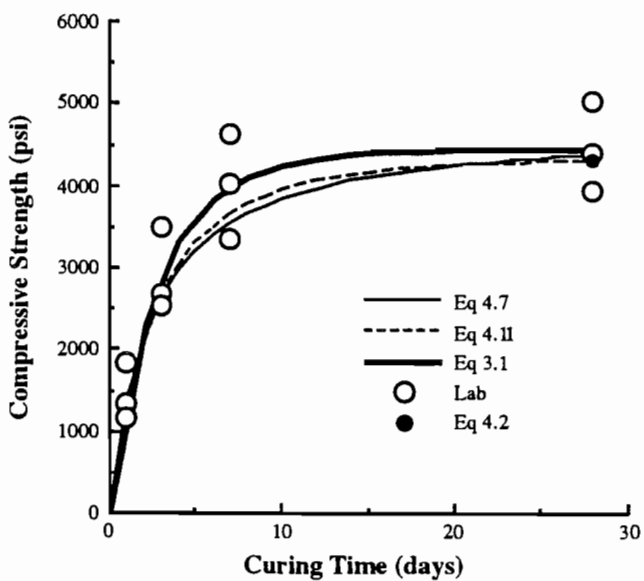


Figure A.1 Compressive strength of dolomite

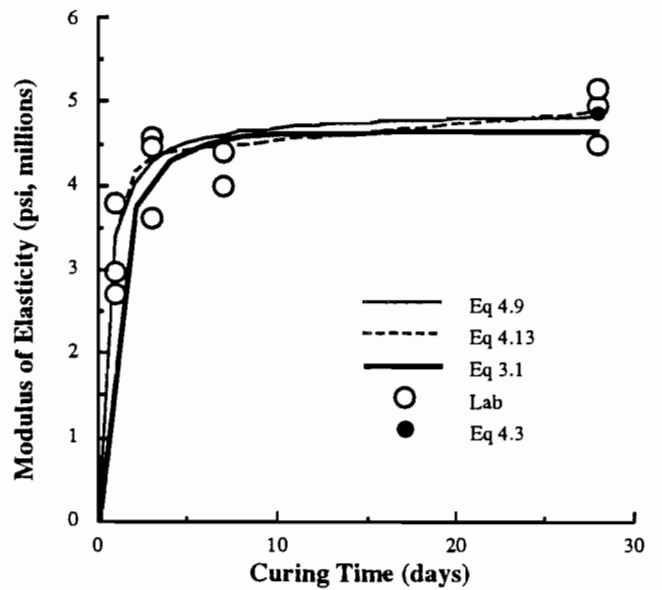


Figure A.3 Elastic modulus of dolomite

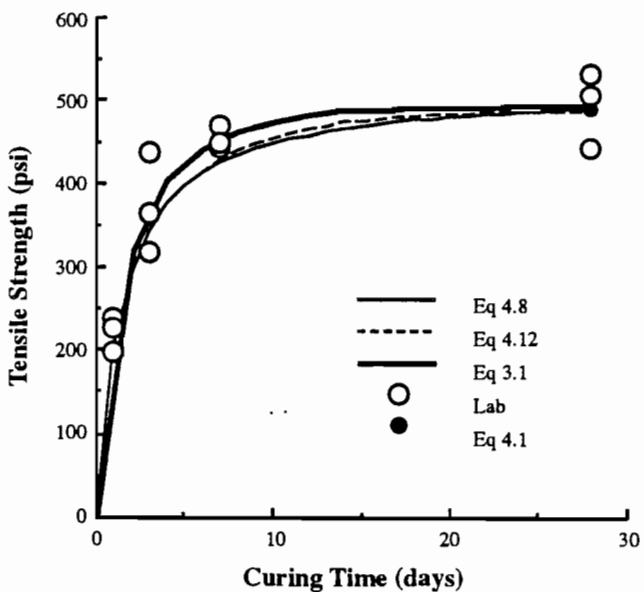


Figure A.2 Tensile strength of dolomite

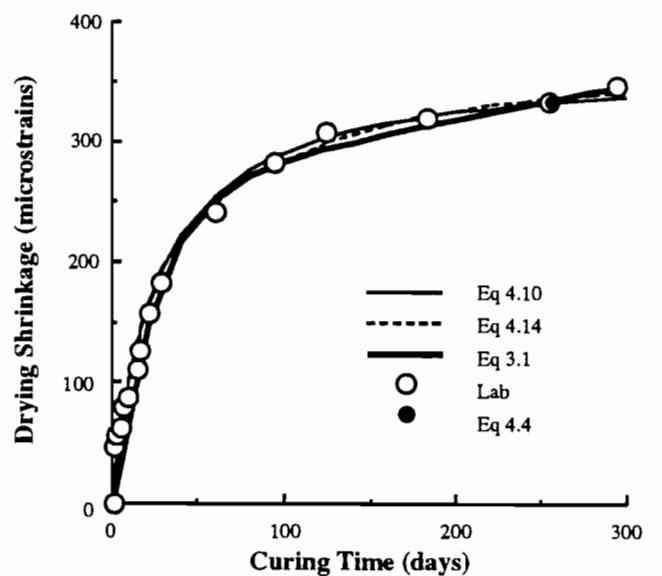


Figure A.4 Drying shrinkage of dolomite

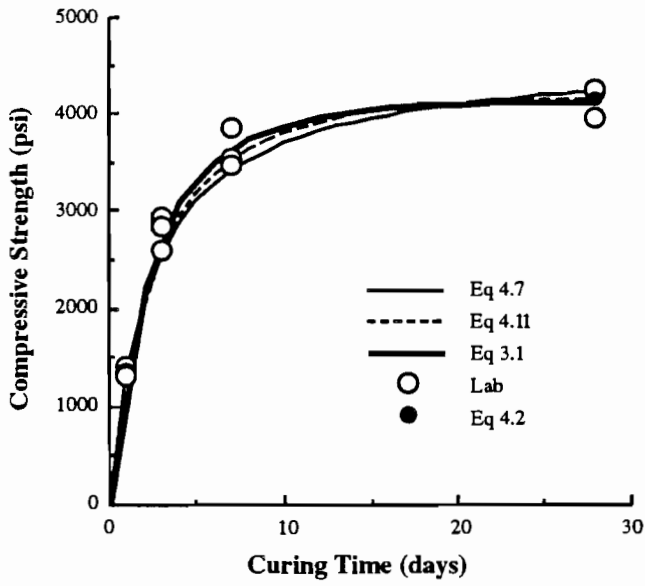


Figure A.5 Compressive strength of Western Tascosa

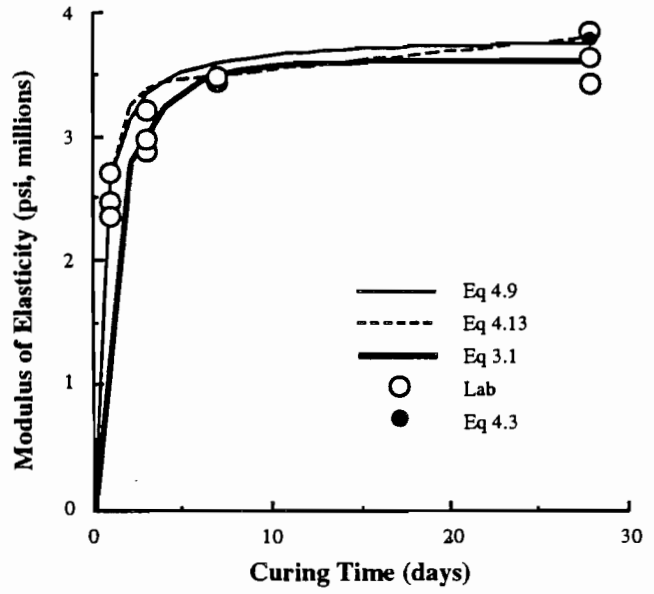


Figure A.7 Elastic modulus of Western Tascosa

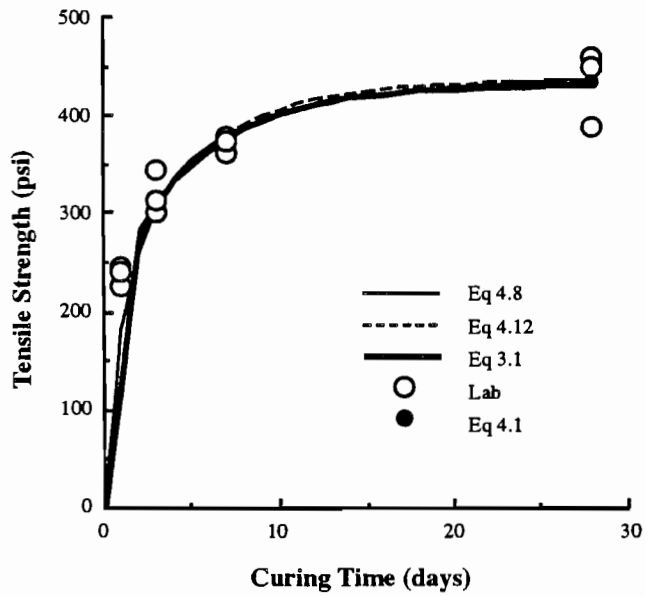


Figure A.6 Tensile strength of Western Tascosa

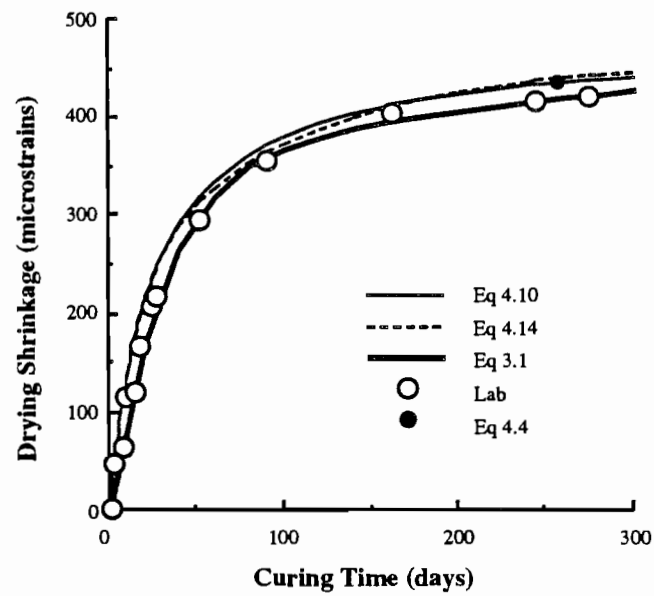


Figure A.8 Drying shrinkage of Western Tascosa

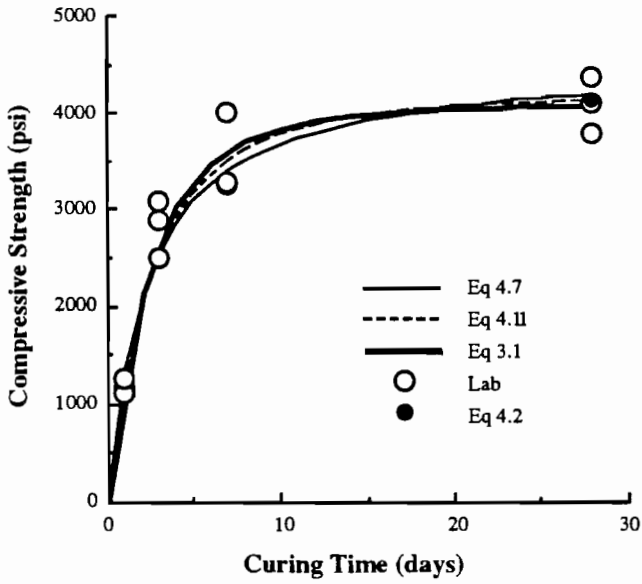


Figure A.9 Compressive strength of Bridgeport/Tin Top

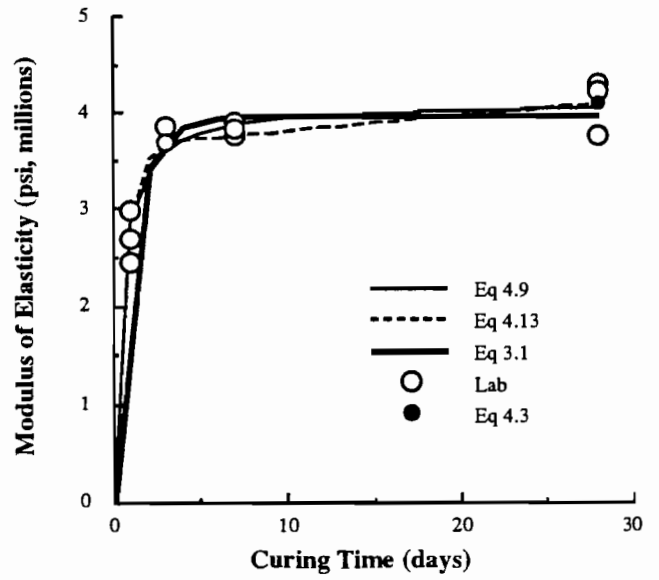


Figure A.11 Elastic modulus of Bridgeport/Tin Top

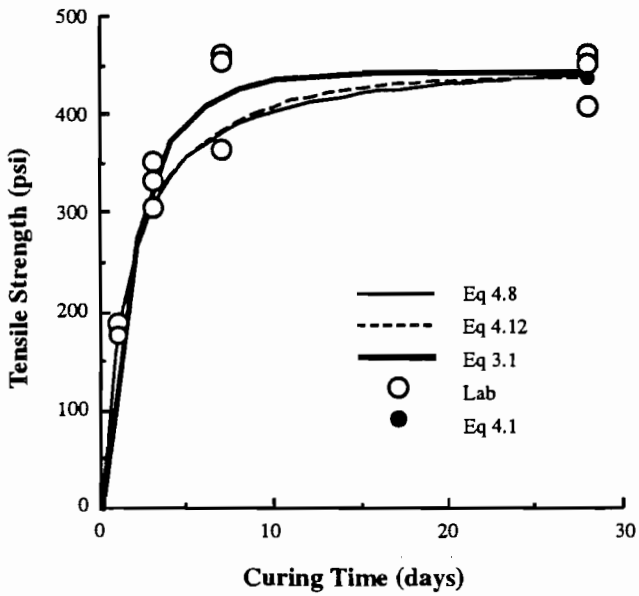


Figure A.10 Tensile strength of Bridgeport/Tin Top

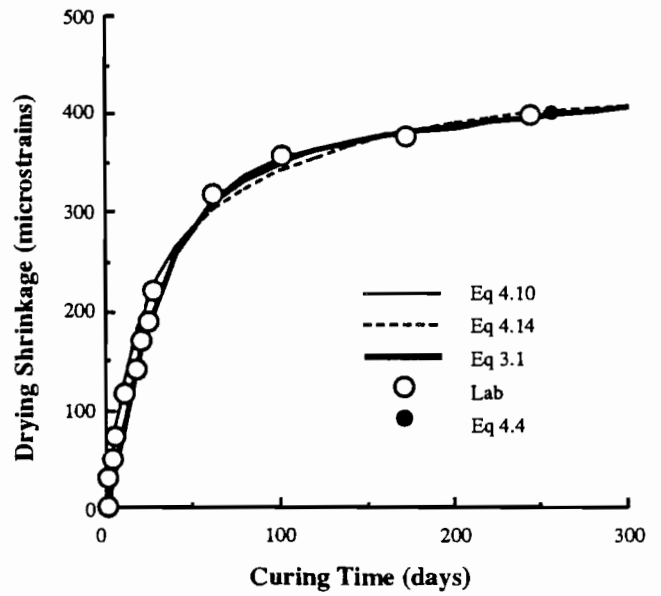


Figure A.12 Drying shrinkage of Bridgeport/Tin Top

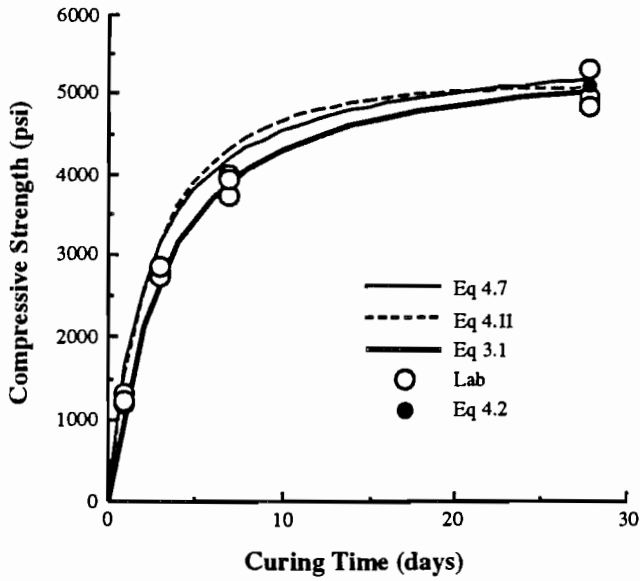


Figure A.13 Compressive strength of limestone

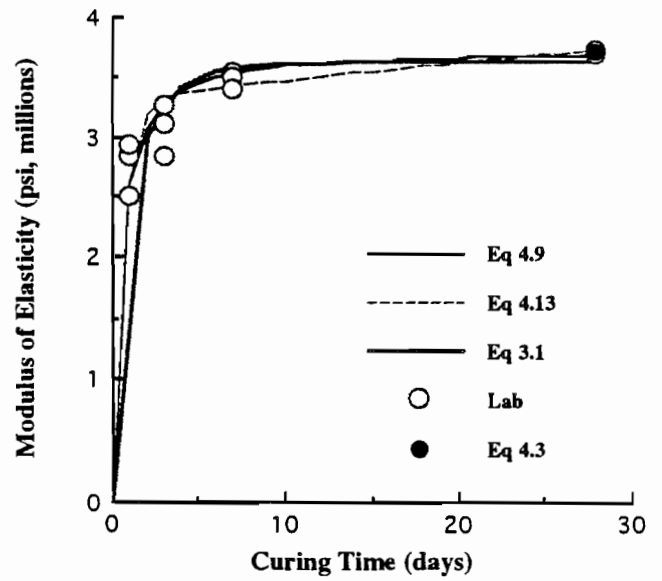


Figure A.15 Elastic modulus of limestone

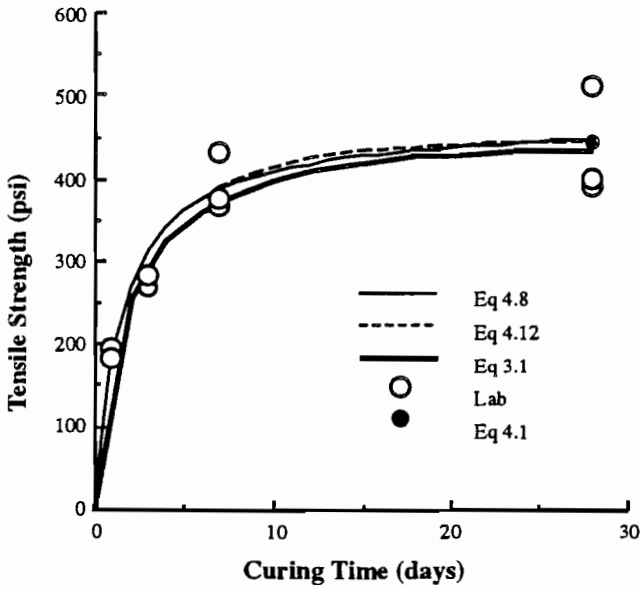


Figure A.14 Tensile strength of limestone

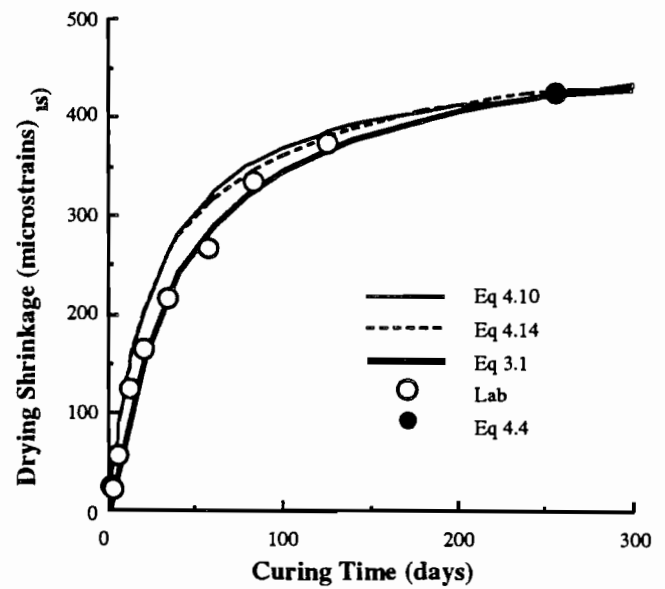


Figure A.16 Drying shrinkage of limestone

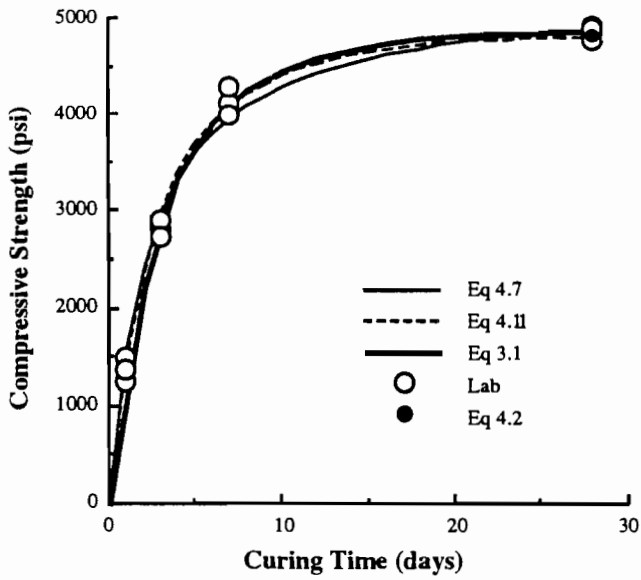


Figure A.17 Compressive strength of siliceous river gravel

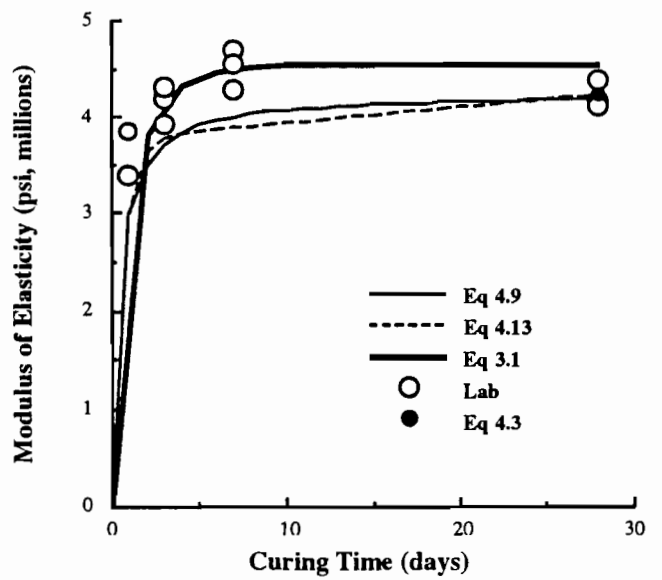


Figure A.19 Elastic modulus of siliceous river gravel

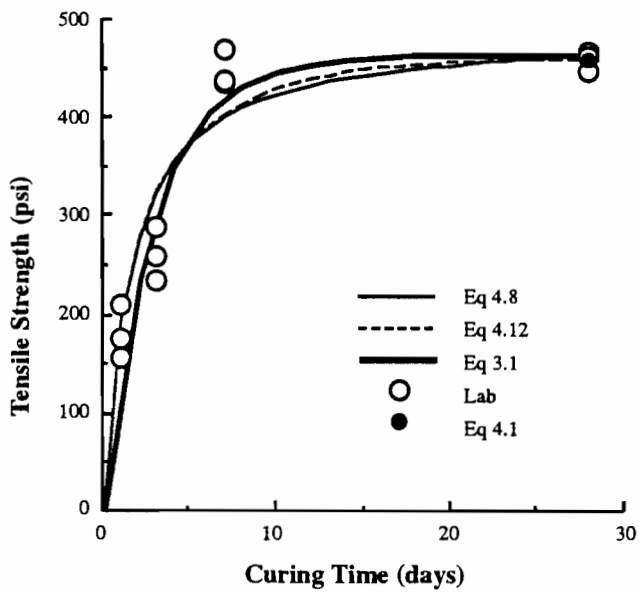


Figure A.18 Tensile strength of siliceous river gravel

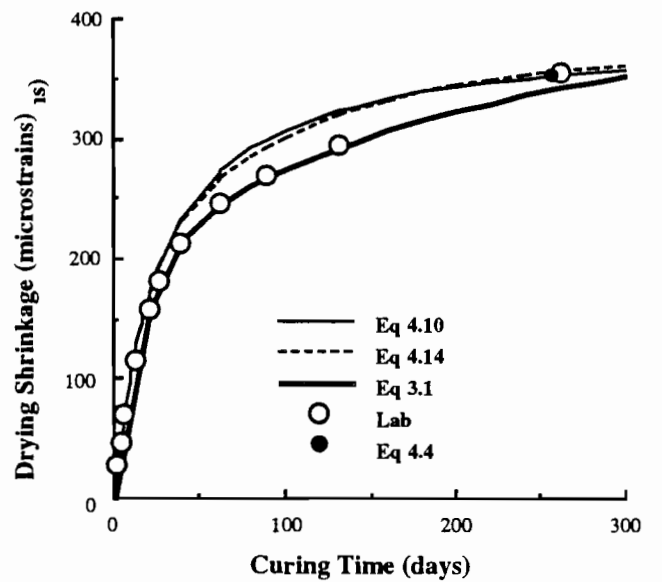


Figure A.20 Drying shrinkage of siliceous river gravel

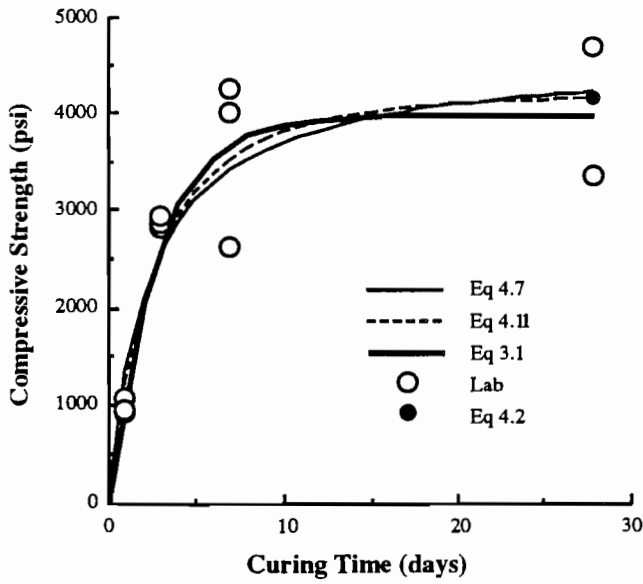


Figure A.21 Compressive strength of Vega

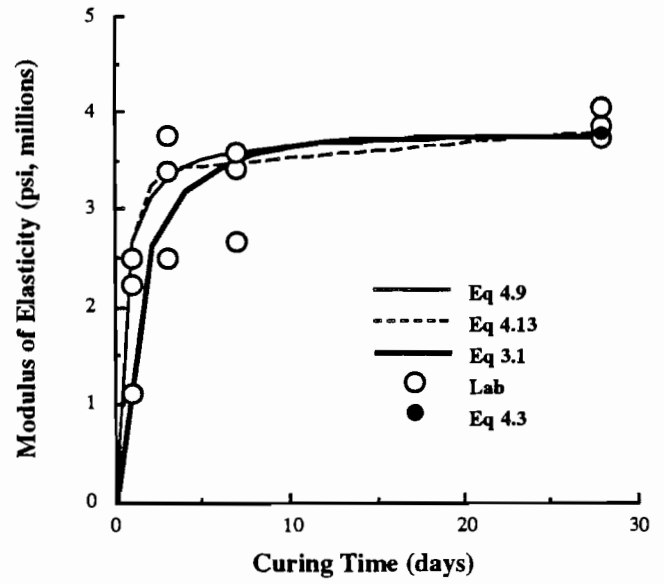


Figure A.23 Elastic modulus of Vega

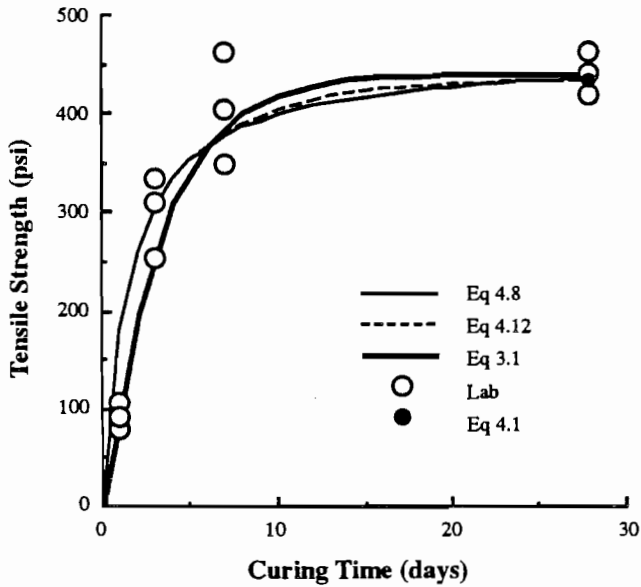


Figure A.22 Tensile strength of Vega

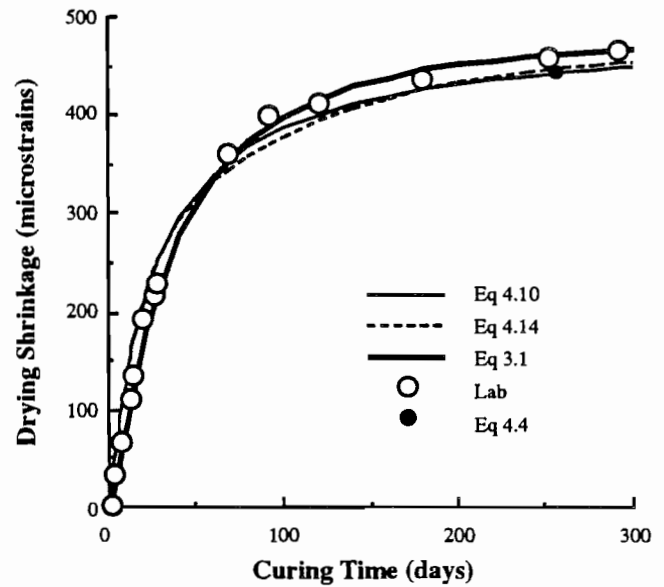


Figure A.24 Drying shrinkage of Vega

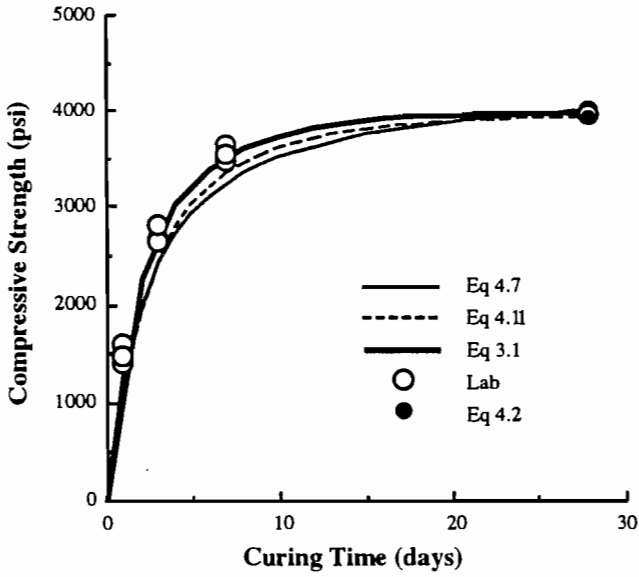


Figure A.25 Compressive strength of Ferris

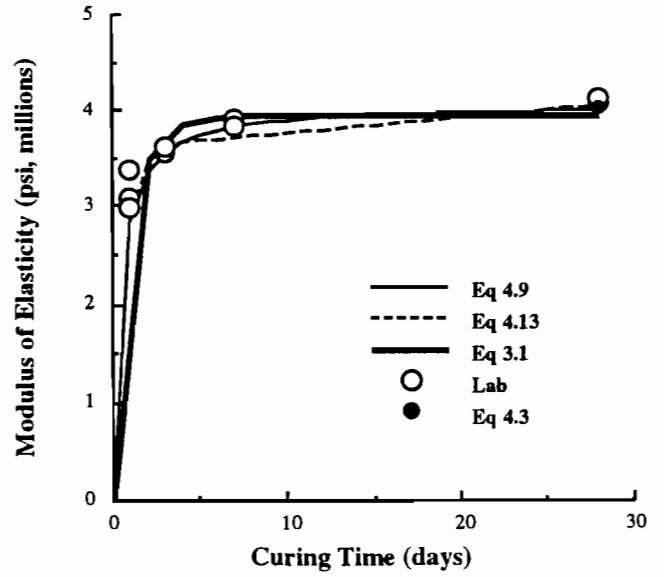


Figure A.27 Elastic modulus of Ferris

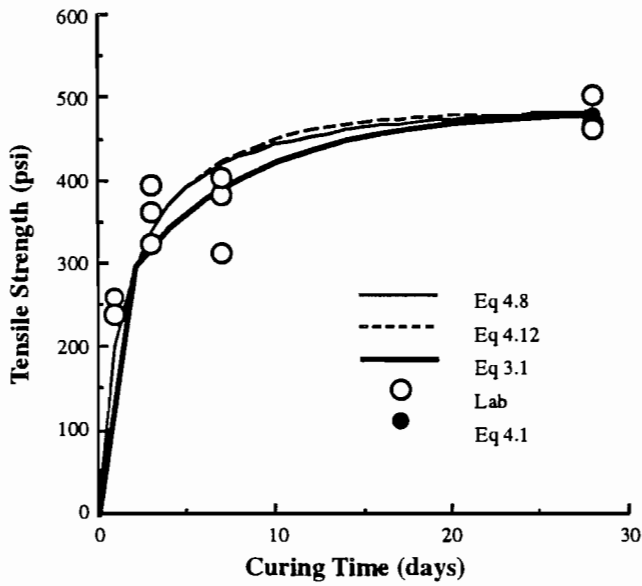


Figure A.26 Tensile strength of Ferris

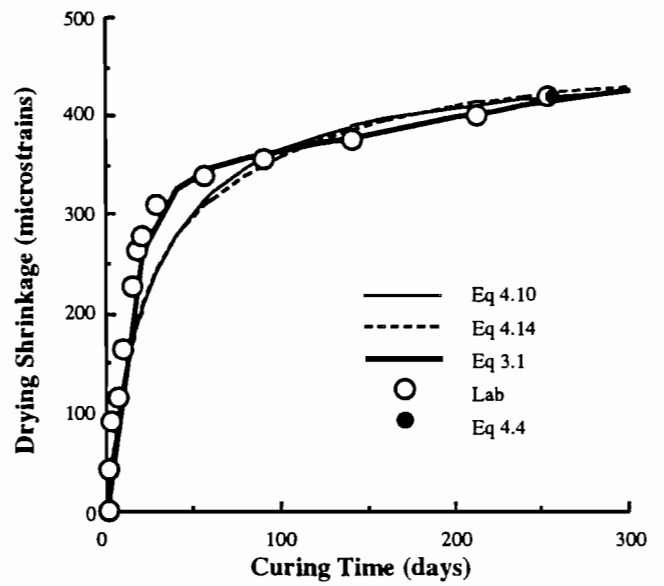


Figure A.28 Drying shrinkage of Ferris

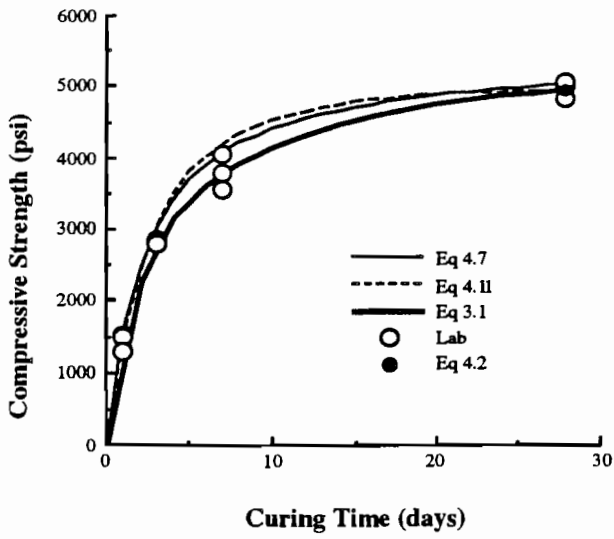


Figure A.29 Compressive strength of granite

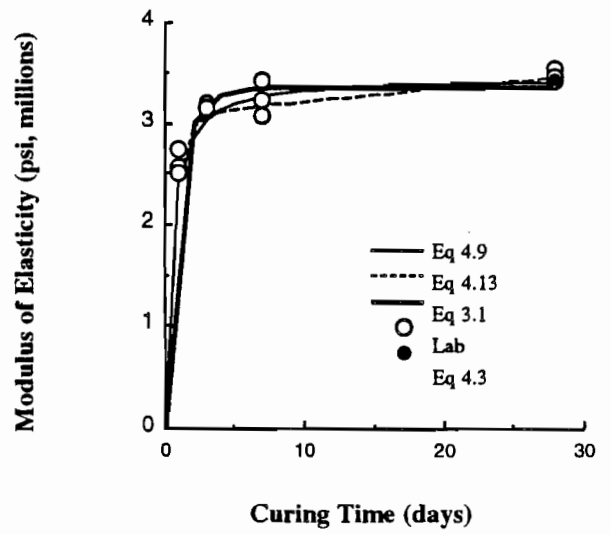


Figure A.31 Elastic modulus of granite

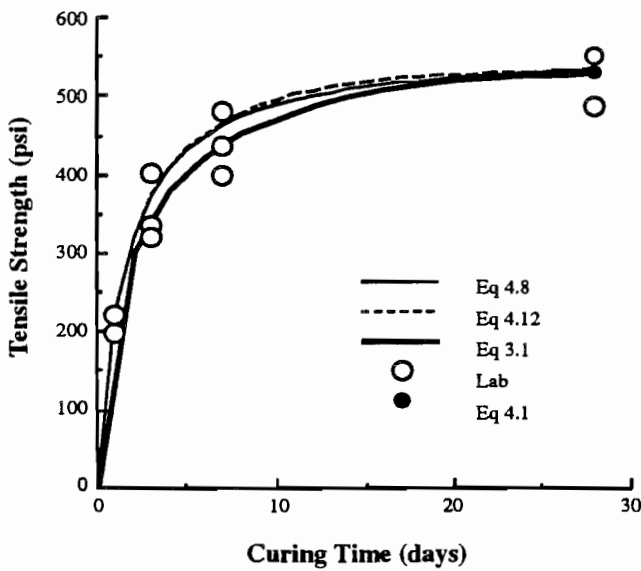


Figure A.30 Tensile strength of granite

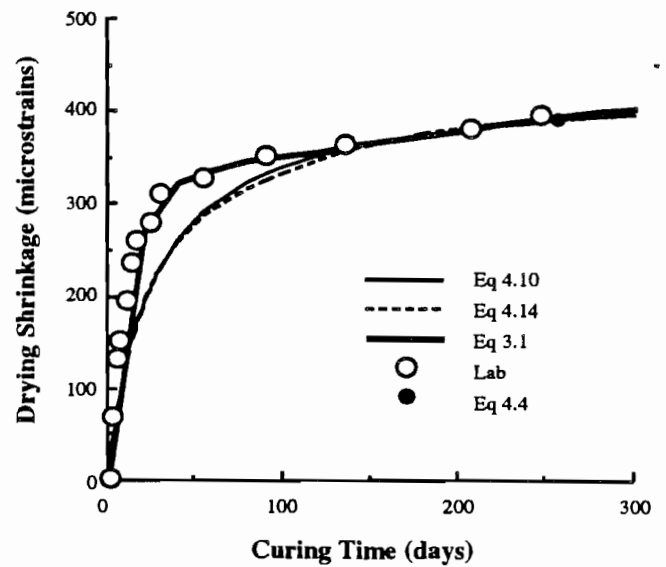


Figure A.32 Drying shrinkage of granite

APPENDIX B. REGRESSION MODEL PROGRAMS

Table B.1 SAS program to model 28 day properties

```
GOPTIONS DEVICE=TEK4105 GPROTOCOL=GSAS7171;
/****422 CHEM ANAL, FINAL METHOD, TM 422-?? *****/
OPTIONS NODATE REPLACE;
/***** INPUT AGGREGATE CHEMICAL COMPOSITION AND 28 DAY PROPERTIES ***/
CMS FI IN DISK 422CHEM DATA A;
DATA A; INFILE IN;
INPUT AGG D $ SIO2 TIO2 AL2O3 FE2O3 MNO MGO CAO NA2O K2O CO2 FC FT E Z;
RUN; TITLE 'TABLE 1. CHEMICAL COMPOSITION OF AGGREGATES';
PROC PRINT; RUN;
/***** INVESTIGATE CORRELATIONS BETWEEN CHEMICAL COMPONENTS *****/
TITLE 'TABLE 2. CORRELATIONS BETWEEN CHEMICAL COMPONENTS';
PROC CORR; VAR SIO2 TIO2 AL2O3 FE2O3 MNO MGO CAO NA2O K2O CO2;
/***** CALCULATE INTERACTIONS AND LOGS OF CHEMICALS *****/
DATA SDS.B; SET A;
I1=SIO2*CAO;I2=SIO2*MGO;I3=SIO2*AL2O3;I4=SIO2*FE2O3;
I5=CAO*MGO; I6=CAO*AL2O3; I7=CAO*FE2O3;
I8=MGO*AL2O3; I9=MGO*FE2O3;
I10=AL2O3*FE2O3;
R1=SIO2/CAO;R2=SIO2/MGO;R3=SIO2/AL2O3;R4=SIO2/FE2O3;
R5=CAO/MGO; R6=CAO/AL2O3; R7=CAO/FE2O3;
R8=MGO/AL2O3; R9=MGO/FE2O3; R10=AL2O3/FE2O3;
SIO2=LOG(SIO2); TIO2=LOG(TIO2); AL2O3=LOG(AL2O3); FE2O3=LOG(FE2O3);
MNO=LOG(MNO); MGO=LOG(MGO); CAO=LOG(CAO); NA2O=LOG(NA2O); K2O=LOG(K2O);
CO2=LOG(CO2);LFT=LOG(FT);LFC=LOG(FC);LE=LOG(E);LZ=LOG(Z); RUN;
/***** FIND BEST 3 VARIABLE MODELS *****/
TITLE 'TABLE 6. POSSIBLE REGRESSION MODELS FOR DRYING SHRINKAGE';
PROC RSQUARE;
MODEL FT FC E Z=I5-I10 R5-R10 CAO MGO AL2O3 FE2O3/STOP=3 SELECT=5;
/***** FIND COEFFICIENTS FOR SELECTED MODELS *****/
TITLE 'TABLE 10. COEFFICIENTS FOR DRYING SHRINKAGE MODEL';
PROC GLM; MODEL Z=CAO MGO R5/SOLUTION;
OUTPUT OUT=C P=PRED R=RESID; RUN;
PROC GPLOT; PLOT PRED*Z; RUN;
PROC PRINT; VAR AGG D PRED Z RESID;
```

Table B.2 SAS program to estimate time coefficients

```
/***** TM 422-? CALCULATE CURING SHAPES FROM CONCRETE DATA *****/
GOPTIONS DEVICE=TEK4105 GPROTOCOL=GSAS7171;
OPTIONS REPLACE;
DATA A;SET SDS.C; IF NOT (T=0);
PROC PRINT;RUN;
PROC NLIN BEST=1;
/*PARMS A=2 TO 5 BY 1
      B=.5 TO 1 BY .1 ;
MODEL Z= Z28*(T/(A+B*T));
      PARMS A=.8 TO 1.5 BY .1
      B= 300 TO 500 BY 50;
MODEL Z=A* Z28-B/T; */
PARMS A=.8 TO 1.5 BY .1
      B=0 TO 2 BY .1;
MODEL Z=A* Z28*(1-EXP(-B*T)); /*
PARMS A=0 TO 5 BY 1
      B= 0 TO 20 BY 5
      C= 0 TO 20 BY 5;
MODEL Z=A* Z28*(2-EXP(-B*T)-EXP(-C*T)); */
OUTPUT OUT=XYZ P=PRED R=RESID ;
TITLE 'PREDICTED VALUES AND RESIDUALS';
PROC PRINT; VAR AGG T Z PRED RESID CS28 TS28 E28 Z28;
```

APPENDIX C. CHEM COMPUTER PROGRAM LISTING (V 1.0)

```
04 REM
05 REM ***** BASIC PROGRAM TO ESTIMATE CONCRETE PROPERTIES FROM CHEMICAL COMPOSITION
DATA *****
06 REM
10 DIM FC(112), ft(30), e(112), z(256), DAT$(10), YROW(10), XCOL(10), DATL(10)
20 DIM XFAK(10), REP(10), x(256), y(256): CLEAR : SHELL "graphics"
22 REM***Test and adjust for EGA or CGA graphics*****
23 sm0 = 9: ON ERROR GOTO 24: SCREEN 9: ON ERROR GOTO 0: GOTO 25
24 sm0 = 2
25 REM***** PRINT FIRST DISCLAIMER SCREEN *****
30 SCREEN 1: WIDTH 80: SCREEN 0: COLOR 15, 1, 1: CLS
32 LOCATE 4, 26: PRINT "PROGRAM CHEM - Version 1.0 "
34 LOCATE 5, 28: PRINT "T. Dossey & B. Black"
36 LOCATE 6, 35: PRINT "9/19/89"
38 LOCATE 10, 13: PRINT "This program was developed by The Center for Transportation"
41 LOCATE 12, 8: PRINT "Research at The University of Texas to predict concrete material"
44 LOCATE 14, 8: PRINT "properties from aggregate chemical composition, based on a model"
45 LOCATE 16, 8: PRINT "documented in CTR report 422/1244-1. It is intended as a comparative"
50 LOCATE 18, 8: PRINT "tool only, and no warranty of these predictions is expressed or"
52 LOCATE 20, 8: PRINT "implied.":
59 LOCATE 22, 27: PRINT "<Press any key to continue>"
80 GOSUB 15000: REM**** wait for keypress *****
100 REM***** CHEMICAL INPUT SCREEN *****
105 CLS : SCREEN 1: WIDTH 80: SCREEN 0: COLOR 15, 1, 8: CLS : LOCATE 6, 10
110 LOCATE 6, 15: PRINT "Enter the percentage by weight of each chemical component"
130 LOCATE 7, 10: PRINT "in the appropriate field. Use the cursor keys (up and down) to"
150 LOCATE 8, 10: PRINT "move between the fields."
160 LOCATE 10, 10: PRINT "Aggregate type          ":
170 LOCATE 12, 10: PRINT "Percent CaO          "
180 LOCATE 14, 10: PRINT "Percent MgO          "
190 LOCATE 16, 10: PRINT "Percent Al2O3        "
200 LOCATE 18, 10: PRINT "Percent Fe2O3        "
210 LOCATE 23, 28: PRINT "<PRESS ENTER TO CONTINUE>"
230 *****INPUT ROUTINE*****
240 DAT$(1) = STRING$(30, "_"): DATL(1) = 29: XCOL(1) = 40: YROW(1) = 10
250 FOR i = 2 TO 5: DAT$(i) = "_____": DATL(i) = 4: XCOL(i) = 40: NEXT i
280 YROW(2) = 12: YROW(3) = 14: YROW(4) = 16: YROW(5) = 18
320 J = 1: K = 5: SCR = 1: SKUP = 1: skdn = 1
325 GOSUB 6830: REM***** call input subroutine *****
2030 cao = VAL(DAT$(2)): mgo = VAL(DAT$(3)): al2o3 = VAL(DAT$(4))
2060 fe2o3 = VAL(DAT$(5))
2061 FOR i = 1 TO 30
2062 A$ = MID$(DAT$(1), i, 1)
2063 n = ASC(A$)
2064 IF n = 95 THEN agg$ = MID$(DAT$(1), 1, i - 1): i = 30
```

```

2066 NEXT i
2120 REM***** PLOT COMPRESSIVE STRENGTH *****
2130 fc28 = -403.1599 * LOG(cao) + 6.80615 * (cao / al2o3) + 5120.548
2140 FOR i = 1 TO 112: x(i) = (i - 1) / 4
2150 FC(i) = fc28 * (x(i) / (2.1743 + .90597 * x(i))):
2160 y(i) = FC(i): NEXT i: xl = 0: xh = 30: xg = 5
2170 n = 112: yh = INT(y(112) / 1000 + .999) * 1000: IF yh < 5000 THEN yh = 5000
2175 yl = yh - 5000: xs = 2: sm = sm0
2180 gt$ = "PREDICTED Fc FOR " + agg$: yg = 1000
2190 yl$ = "Compr Strength PSI": xl$ = "Curing Time (days)"
2200 GOSUB 16000: REM**** call plot routine *****
2210 GOSUB 17000: REM**** Hardcopy of Plot? *****
2570 REM***** plot tensile strength curve *****
2580 ft28 = -59.23776 * LOG(cao) + 46.88364 * LOG(mgo) + 1.715897 * (cao / mgo) + 572.15169#
2590 FOR i = 1 TO 28: x(i) = i - 1
2600 ft(i) = ft28 * (x(i) / (1.43139 + .94156 * x(i)))
2610 y(i) = ft(i): NEXT: n = 28: xl = 0: xh = 30: yh = INT(ft28 / 100 + .99) * 100
2620 IF yh < 500 THEN yh = 500
2622 yl = yh - 500: yg = 100: xg = 5
2630 xl$ = "Curing Time (days)": yl$ = "Tens Strength PSI"
2635 gt$ = "Predicted Ft for " + agg$: xs = 2: GOSUB 16000
3010 GOSUB 17000: REM**** Hardcopy of Plot? *****
3000 REM***** plot elastic modulus curve *****
3030 e28 = -.41348538# * LOG(al2o3) + .263987 * LOG(mgo) - 9.48304E-03 * (cao / al2o3) + 4.6642985#
3040 FOR i = 1 TO 112: x(i) = (i - 1) / 4
3050 e(i) = e28 * (x(i) / (.43056 + .99451 * x(i)))
3060 y(i) = e(i): NEXT: n = 112: xl = 0: xh = 30: yh = INT(e28 + .99)
3065 IF yh < 5 THEN yh = 5
3067 yl = yh - 5: yl$ = "Elas Mod Millions": yg = 1
3068 gt$ = "Predicted E for " + agg$: xs = 2: xl$ = "Curing Time (days)": GOSUB 16000
3495 GOSUB 17000: REM***** Hardcopy of Plot *****
3500 REM***** plot drying shrinkage *****
3520 z256 = 1.8723354# * (cao * al2o3) + .122303 * (cao / fe2o3) - .1383038 * (cao * mgo) + 350.588997#
3530 FOR i = 1 TO 256: x(i) = i - 1
3540 z(i) = z256 * (x(i) / (23.85053 + .910564 * x(i)))
3550 y(i) = z(i): NEXT: n = 256: xh = 300: yh = INT(z256 / 100 + .99) * 100
3555 xl$ = "Curing Time (days)": IF yh < 500 THEN yh = 500
3557 yl = yh - 500: yl$ = "Shrinkage in/in": yg = 100: xg = 50
3558 gt$ = "Predicted Z for " + agg$: xs = 2: GOSUB 16000
3915 GOSUB 17000: REM***** Hardcopy of Plot? *****
3930 SCREEN 0: COLOR 15, 1: CLS
3940 LOCATE 6, 10
3950 PRINT " If you would like to print a summary table of the "
3960 LOCATE 8, 10
3970 PRINT "calculations, turn the printer on and type Y. If not"
3980 LOCATE 10, 10
3990 PRINT "type N."
4000 GOSUB 15100: REM *** yes or no ***
4040 IF t = 0 THEN COLOR 15, 0: CLS : GOTO 4065
4050 IF t = 1 THEN GOSUB 12000: COLOR 15, 0: CLS : GOTO 4065
4060 GOTO 4000
4065 COLOR 15, 1: CLS : LOCATE 5, 10
4070 PRINT "Another aggregate? (Y or N)": GOSUB 15100: IF t = 1 THEN GOTO 100
4080 END
6830 REM***** INPUT SUBROUTINE *****
6840 WIDTH 80: SCREEN 0: COLOR 15, 3, 8
6850 REP(SCR) = 1

```

```

6860 FOR i = J TO K
6870 LOCATE YROW(i), XCOL(i)
6880 COLOR 15, 3, 8
6890 PRINT DAT$(i)
6900 NEXT i
6910 COLOR 15, 3, 8
6920 i = J
6930 REM*****
6935 XFAK(i) = XCOL(i)
6940 IF i < J THEN REP(SCR) = 1: SCR = SCR - 1: REP(SCR) = 1: GOTO 7260
6950 IF i = K + 1 THEN RETURN
6960 IF XFAK(i) < XCOL(i) THEN p = 1: i = i - 1: GOTO 6930
6970 IF XFAK(i) > XCOL(i) + DATL(i) THEN p = -1: i = i + 1: GOTO 6930
6980 y$ = " ": U$ = " "
6990 IF XFAK(i) = 0 THEN XFAK(i) = 1
7000 LOCATE YROW(i), XFAK(i), 1, 0, 7
7010 d$ = INKEY$: z = LEN(d$): IF z = 0 THEN GOTO 7010
7040 r$ = RIGHT$(d$, 1)
7050 r = ASC(r$)
7070 IF z = 1 THEN GOTO 7130
7072 IF r = 59 THEN 2030
7074 IF r = 79 THEN 2030
7076 IF r = 81 THEN SCR = SCR + 1: GOTO 7255
7078 IF r = 71 THEN SCR = 0: GOTO 7255
7080 IF r = 75 THEN XFAK(i) = XFAK(i) - 1: GOTO 6960
7090 IF r = 77 THEN XFAK(i) = XFAK(i) + 1: GOTO 6960
7100 IF r = 72 THEN p = SKUP: i = i - SKUP
7110 IF r = 80 THEN p = -skdn: i = i + skdn
7115 IF r = 9 THEN p = -skdn: i = i + skdn
7120 GOTO 6930
7130 IF r = 13 THEN p = -1: i = i + 1: GOTO 6930
7135 IF r = 9 THEN p = -1: i = i + 1: GOTO 6930
7140 IF r = 8 THEN XFAK(i) = XFAK(i) - 1: GOTO 6960
7150 PRINT d$
7160 C = LEN(DAT$(i))
7170 n = XFAK(i) - XCOL(i)
7180 IF C < n THEN DAT$(i) = DAT$(i) + d$: XFAK(i) = XFAK(i) + 1: GOTO 6960
7190 IF C = n THEN DAT$(i) = DAT$(i) + d$: XFAK(i) = XFAK(i) + 1: GOTO 6960
7200 O = C - n - 1
7210 U$ = RIGHT$(DAT$(i), O)
7220 y$ = LEFT$(DAT$(i), n)
7230 DAT$(i) = y$ + d$ + U$
7240 XFAK(i) = XFAK(i) + 1
7250 GOTO 6960
7255 'NULL
7260 GOTO 100
7300 END
12000 REM ***** PRINT RESULTS ON PRINTER SUBROUTINE *****
12001 LPRINT CHR$(12); STRING$(80, "**")
12002 LPRINT TAB(23); "Prediction of Concrete Properties"
12003 LPRINT TAB(38); "from "
12004 LPRINT TAB(19); " Chemical Composition of Coarse Aggregate": LPRINT " "
12005 LPRINT STRING$(80, "**"): LPRINT : LPRINT " Aggregate: "; agg$: LPRINT
12006 f1$ = " ": IF (cao > 45.7) OR (cao < 1.5) THEN f1$ = "**"
12007 f2$ = " ": IF (mgo > 13) OR (mgo < .11) THEN f2$ = "**"
12008 f3$ = " ": IF (al2o3 > 14.3) OR (al2o3 < .21) THEN f3$ = "**"
12009 f4$ = " ": IF (fe2o3 > 3.7) OR (fe2o3 < .06) THEN f4$ = "**"

```



```

12010 LPRINT USING " Calcium Oxide: ##.##"; cao; : LPRINT " % "; f1$
12012 LPRINT USING "Magnesium Oxide: ##.##"; mgo; : LPRINT " % "; f2$
12015 LPRINT USING " Aluminum Oxide: ##.##"; al2o3; : LPRINT " % "; f3$
12020 LPRINT USING " Ferrrous Oxide: ##.##"; fe2o3; : LPRINT " % "; f4$: LPRINT
12025 LPRINT : LPRINT "Prediction of Properties": LPRINT STRING$(24, "-")
12030 LPRINT " ": s$ = SPACE$(10)
12090 LPRINT " Age", "Compressive", " Tensile", "Elastic Mod.", " Shrinkage"
12091 LPRINT "(days)", "Strength-PSI", "Strength-PSI", "(PSI x 10^6", "(in/in x 10^-6)"
12093 LPRINT "_____", "_____", "_____", "_____", "_____"
12100 LPRINT USING " 1" + s$ + "#####" + s$ + "####" + s$ + "##.##" + s$ + "####"; FC(5); ft(2); e(5);
z(2)
12110 LPRINT USING " 3" + s$ + "#####" + s$ + "####" + s$ + "##.##" + s$ + "####"; FC(13); ft(4); e(13);
z(4)
12120 LPRINT USING " 7" + s$ + "#####" + s$ + "####" + s$ + "##.##" + s$ + "####"; FC(29); ft(8); e(29);
z(8)
12130 LPRINT USING " 28" + s$ + "#####" + s$ + "####" + s$ + "##.##" + s$ + "####"; FC(112); ft(28);
e(112); z(29)
12140 LPRINT USING " 256" + s$ + " ." + s$ + " ." + s$ + " ." + s$ + "####"; z(256)
12150 IF f1$ = " " AND f2$ = " " AND f3$ = " " AND f4$ = " " THEN GOTO 12170
12160 LPRINT : LPRINT : LPRINT CHR$(14); "**** WARNING! ****": LPRINT
12165 LPRINT " Chemicals flagged with (*) are present in amounts not found in"
12166 LPRINT " any aggregate used in model development. Results may be incorrect."
12170 REM***** print disclaimer *****
12175 FOR i = 1 TO 12: LPRINT : NEXT: LPRINT STRING$(80, "**")
12178 LPRINT " Program developed by T. Dossey and B. Black according to model presented"
12180 LPRINT "in CTR report 422/1244-1. These predictions are meant for comparison purposes"
12190 LPRINT "only, and no warranty of their accuracy is stated or implied."
12500 RETURN
15000 REM***** wait for keypress *****
15010 IF 0 = LEN(INKEY$) THEN 15010 ELSE RETURN
15100 REM***** Yes or No Subroutine *****
15110 t = 0: d$ = INKEY$: z = LEN(d$): IF z = 0 THEN 15110
15120 IF d$ = "Y" OR d$ = "y" THEN t = 1
15130 RETURN
16000 REM***** FULL SCREEN PLOT ROUTINE *****
16002 REM** x and y are points to be plotted
16003 REM** n is number of points
16004 REM** xl and yl are x and y lower WINDOW limits
16005 REM** xh and yh are x and y upper WINDOW limits
16006 REM** xl$ is x axis label, yl$ is y axis label
16007 REM** vertical grids at xg, horiz grids at yg, 0 for none
16008 REM** gt$ is the graph title, at the top
16009 REM** xs is 1 for label every x tic, 2 for every other, etc
16010 REM** SM is screen mode, 9 for hi-res, 2 for printer plot
16013 SCREEN 0: CLS : SCREEN sm:
16015 IF sm = 9 THEN COLOR 15, 1: VIEW (93, 62)-(563, 272), , 15
16016 IF sm = 2 THEN VIEW (93, 35)-(563, 155), , 15:
16017 WINDOW (xl, yl)-(xh, yh): CLS
16020 REM***** draw plot line *****
16030 FOR i = 1 TO n - 1: LINE (x(i), y(i))-(x(i + 1), y(i + 1)): NEXT
16040 REM***** draw vertical grid lines *****
16050 IF xg = 0 THEN GOTO 16080: REM*** no vert. grid lines ***
16060 nl = INT((xh - xl) / xg) - 1
16070 FOR i = 1 TO nl: LINE (xg * i, yl)-(xg * i, yh), , &H8888: NEXT
16080 REM***** draw horizontal grid lines *****
16085 IF yg = 0 THEN GOTO 16110: REM*** no horiz grid lines ****
16090 nl = INT((yh - yl) / yg) - 1

```

```

16100 FOR i = 1 TO nl: LINE (xl, yl + yg * i)-(xh, yl + yg * i), , , &H8888: NEXT
16110 REM***** draw graph title *****
16115 l = LEN(gt$): LOCATE 2, 40 - INT(l / 2): PRINT gt$
16130 REM***** draw x axis label *****
16140 l = LEN(xl$): LOCATE 22, 40 - INT(l / 2): PRINT xl$
16150 REM***** label y axis grid lines *****
16160 yinc = 16 / (yh - yl): nl = INT((yh - yl) / yg)
16170 FOR i = 0 TO nl: yy = 15 * yg * i / (yh - yl): y$ = STR$(yl + yg * i)
16175 ll = LEN(y$): LOCATE 20 - INT(.5 + yy), 11 - ll: PRINT y$: NEXT
16180 REM***** draw y axis label *****
16190 l = LEN(yl$): FOR i = 1 TO l: LOCATE i + 12 - INT(l / 2), 8 - ll: PRINT MID$(yl$, i, 1): NEXT
16200 REM***** label x axis grid lines *****
16210 xinc = 60 * xg / (xh - xl): nl = INT((xh - xl) / xg) + 1
16220 FOR i = 1 TO nl STEP xs: x$ = STR$(xl + xg * (i - 1)): l = LEN(x$)
16230 LOCATE 21, xinc * i - l + 3: PRINT x$: NEXT: BEEP: RETURN
17000 REM***** Hardcopy of Plot on Printer *****
17005 LOCATE 24, 22: PRINT "<Press Y for Hardcopy, N to continue>";
17020 GOSUB 15100: IF t = 1 THEN sm = 2: GOSUB 16000: CALL interrupt(5, 2, 2)
17025 sm = sm0: RETURN
17500 REM***** flashing message subroutine *****
17510 l = LEN(M$): s1$ = M$: s2$ = SPACE$(l)
17515 LOCATE 24, 22: PRINT s1$; : FOR i = 1 TO 1000: d$ = INKEY$:
17520 IF LEFT$(d$, 1) = "y" THEN t = 1: RETURN
17530 IF LEN(d$) <> 0 THEN t = 0: RETURN
17540 NEXT: s$ = s1$: s1$ = s2$: s2$ = s$: GOTO 17515

```